Generalized Eigenvector Algorithm for Blind Equalization*

Björn Jelonnek, Dieter Boss, Karl-Dirk Kammeyer

University of Bremen, FB-1, Dept of Telecommunications, P.O. Box 330440, D-28334 Bremen, Germany, Tel.: +(49)-421/218-3356, Fax: -3341, E-mail: boss@comm.uni-bremen.de, http://www.comm.uni-bremen.de

Abstract

In 1994, an eigenvector solution to the problem of blind equalization of possibly mixed-phase linear time-invariant transmission channels was published in this journal. Unfortunately, this solution is ambiguous on a certain condition. In this paper, we introduce a novel iterative method termed EIGENVECTOR ALGORITHM FOR BLIND EQUALIZATION (EVA), which not only overcomes the uniqueness problem, but also ensures, after some iterations, optimum linear equalization *from few samples of the received signal*. In the second part of the paper, the eigenvector solution is generalized to multiple output channels. The resulting algorithm, called GENEVA (GENERALIZED EVA), can be applied to the iterative adjustment of *(i)* multiple parallel symbol-rate FIR equalizers, *(ii)* fractional tap spacing FIR equalizers, *(iii)* non-linear decision-feedback and *(iv)* time-variant FIR equalizers. Extensive simulation results illustrate the exceptional capabilities of GENEVA.

Zusammenfassung

In dieser Zeitschrift wurde 1994 eine Eigenvektor-Lösung zur blinden Entzerrung von evtl. gemischtphasigen, linearen zeitinvarianten Übertragungskanälen veröffentlicht. Unter einer bestimmten Bedingung ist diese Lösung leider mehrdeutig. In diesem Artikel wird nun eine neuartige iterative Methode vorgestellt, die nicht nur das Eindeutigkeitsproblem überwindet, sondern nach einigen Iterationen auch die optimale lineare Entzerrung *auf der Basis von wenigen Abtastwerten des Empfangssignals* sicherstellt. Sie wird EIGENVEKTOR-ALGORITHMUS ZUR BLINDEN ENTZERRUNG (EVA) genannt. Im zweiten Teil des Artikels wird die Eigenvektor-Lösung auf Kanäle mit mehreren Ausgängen verallgemeinert. Der resultierende Ansatz GENEVA (GENERALIZED EVA) kann zur iterativen Einstellung folgender Entzerrerstrukturen verwendet werden: *(i)* mehrere parallele Symboltakt-FIR-Entzerrer, *(ii)* Entzerrer mit Mehrfachabtastung oder *(iii)* quantisierter Rückführung sowie *(iv)* zeitvariante FIR-Entzerrer. Umfangreiche Simulationsergebnisse verdeutlichen seine außergewöhnliche Leistungsfähigkeit.

Résumé

Une solution de type sous-espace au problème de l'égalisation aveugle des canaux de transmission invariants, linéaires, à phase mixte, a été publiée dans ce journal en 1994. Malheureusement, cette solution n'est pas unique dans un certain cas. Dans cet article, nous proposons une nouvelle méthode itérative, appelée EVA (EIGENVECTOR ALGORITHM FOR BLIND EQUALIZATION), qui non seulement résoud ce problème d'unicité, mais qui, après quelques itérations, assure aussi une égalisation linéaire optimale *à partir d'un petit nombre d'échantillons du signal reçu*. Dans la deuxième partie de cet article, la solution sous-espace est généralisée aux canaux multi-sorties. L'algorithme correspondant, noté GENEVA (GENERALIZED EVA), peut être appliqué à l'adaptation itérative d'égaliseurs *(i)* transverses multiples en parallele au rythme symbole, *(ii)* transverses fractionnaires, *(iii)* récursifs avec décision dans la boucle et *(iv)* transverses évolutifs en temps. De nombreux résultats de simulations illustrent les capacités exceptionnelles de l'algorithme GenEVA.

*This work is supported by the German National Science Foundation (DFG-contracts Ka 841/1 and /2).

1 Introduction

Equalization is a classical problem in the field of digital communications. With fast data transmission over multipath radio channels, it is aggravated by the following properties of the unknown channel: *(i)* It is frequency selective, *(ii)* its equivalent discrete-time baseband impulse response may be mixed-phase and *(iii)* in a mobile environment, it is *time-variant* so that the equalizer needs to be adjusted repeatedly (*adaptive equalization,* refer to [27], e.g.). As for the latter property, time-variance of the channel is relatively slow in many applications, so that it can be assumed *time-invariant* over a certain period of time (*piecewise* or *quasi* time-invariant).

Within such a period of time-invariance, state-of-the-art digital communication systems transmit *training sequences* to assist the receiver in adjusting its equalizer. For this purpose, the cross-correlation between the received (corrupted) and the stored (ideal) training sequences is calculated. However, depending on the degree of time-variance, the repeated transmission of training sequences leaves the communication system with an overhead which amounts to 22.4% for the example of *GSM (Global System for Mobile communications* [23]). This overhead capacity could be used for other purposes such as channel coding (thus enhancing overall system performance), if the channel equalization problem was solved without training sequences.

In 1975, Sato [29] raised the topic of *self-recovering* or *blind* equalization, where the fundamental idea is to derive the equalizer characteristics from the received signal only, i.e. *without* access to the channel input signal by means of training sequences. Depending on the different ways to extract information from the received signal, two classes of blind approaches can be distinguished:

- **Class HOS:** When the received signal is sampled at symbol-rate, the resulting sequence is (quasi) stationary. Since second order statistics of a stationary signal are inadequate for the determination of the complete equalizer characteristics (including phase information), class HOS approaches are based either explicitly or implicitly on *Higher Order Statistics (HOS).* Higher order *cumulants* contain the complete information on the channel's (and thus the equalizer's) magnitude and phase provided that the distribution of the channel input signal is non-Gaussian. Excellent overviews on HOS and their applications can be found in [25, 20, 21, 24].

- **Class SOCS:** When the sampling period is a fraction of the symbol period (time diversity), or alternatively, the symbol-rate sampled signals received by several sensors are interleaved (antenna diversity), the resulting sequence is (quasi) *cyclostationary* (assuming that some excess bandwidth is available). Generally, *Second Order Cyclostationary Statistics (SOCS)* are sufficient to retrieve the complete equalizer characteristics, but there are "singular" channel classes which can not be equalized this way. They include channels with common subsystems in all polyphase subchannels (refer to [32, 34, 7] for details).

In a mobile propagation environment, the unknown channel assumes an arbitrary impulse response in any instant of time. Particularly, "singular" and "critical"[1] channels can not be prevented from occurring. Furthermore, from the above quasi-time-invariance assumption for the channel, it follows that the received signal can only be observed in a (short) period of time. In summary, a blind equalization algorithm for an application in mobile communications should satisfy the following requirements:

[1]Channels with zeros 'on' or 'close to' the unit circle of the complex z-plane are called "critical".

R1: Optimum[2] linear or non-linear equalization must be obtained *from few samples of the received signal* (hundreds rather than tens of thousand symbol periods).

R2: R1 should be satisfied for any arbitrary channel (such as "singular" and "critical" channels) ...

R3: ... and if independent stationary additive (possibly colored) Gaussian noise is present.

The algorithms we present in this paper meet the above requirements. They are class HOS approaches based on fourth (and second) order stationary statistics. Notice that second order statistics need to be exploited in order to satisfy requirement R3, because fourth order cumulants are asymptotically insensitive to additive Gaussian noise. As the performance level of SOCS-based methods is heavily affected by "singular" channels [3], such approaches are not considered in this paper (cf. R2).

One of the first blind algorithms was introduced by Godard in 1980 [10]. A more general criterion for blind deconvolution based on a particular fourth order cumulant was presented by Donoho [8], and by Shalvi and Weinstein [30]. From the latter approach, a modified structure of a blind equalizer was derived in [14] where a cascade of first order all-pass systems is combined with a lattice prediction error filter. For phase modulated signals, the Constant Modulus Algorithm was developed [33, 18]. It was applied to multipath FM signals and can be regarded as a specific form of a blind algorithm.
The methods cited above ([10, 8, 30, 14, 33, 18]) employ a *scalar quality function based on a HOS property of the equalizer output*. A considerable drawback of these approaches is the large number of received data samples required for a satisfactory equalization quality (thus violating R1). This lack of *convergence rate*, i.e. the rate of improvement in equalization quality as the number of received samples is increased, is due to the simple stochastic gradient method used to optimize the quality function.

Consider two classical algorithms which are frequently applied to determine the optimum solution to (non-blind) linear equalization. The most popular method, called Least Mean Squares (LMS) approach, uses a stochastic gradient search and is rather slow. On the other hand, the Recursive Least Squares (RLS) algorithm converges very quickly. Originally, we have attributed this to the fact that it performs an iterative update of the *closed-form* solution. For *blind* linear equalization, a closed-form expression in guise of an eigenvector problem was found in 1994 [16], where the solution was termed "EVA solution". Similar to RLS, we present in the first part of this paper an approach termed EigenVector Algorithm for blind equalization (EVA) which also updates a closed-form solution iteratively. Its main features are:

F1: After some iterations, EVA converges to the optimum linear equalizer solution. It exhibits an excellent convergence, i.e. it requires a modest number of received data samples. For constant modulus signals, our *blind* approach is shown to converge as fast as the *non-blind* RLS algorithm.

F2: This holds for any linear (quasi) time-invariant channel with finite or infinite impulse response

F3: ... as well as in presence of independent stationary additive (possibly colored) Gaussian noise.

Emphasis must be put on the fact that the pure existence of a closed-form expression can *not* justify EVA's convergence speed. Although EVA was devised in the spirit that RLS' brilliant convergence behavior is due to the iterative update of a closed-form solution, it turned out at a later stage that

[2]Throughout the paper, "optimum" is meant in the minimum *mean square error (MSE)* sense.

the convergence speed of both RLS and EVA is caused by cancellation effects of the correlation (and cumulant) estimation errors within the respective system of equations (see section 3, Figure 5).

It is well known that other equalizer structures are capable of offering performances superior to the optimum linear equalizer [27]. Moreover, the single output channel model used with EVA is not suitable for some applications. Therefore, we generalize the EVA solution to multiple output channels in the second part of this paper. The resulting algorithm, called GenEVA (Generalized EVA), can be applied to the iterative adjustment of *(i)* multiple parallel symbol-rate FIR equalizers, *(ii)* fractional tap spacing FIR equalizers, *(iii)* non-linear decision-feedback and *(iv)* time-variant FIR equalizers.

Note that EVA and GenEVA are genuine equalization algorithms which directly calculate the equalizer coefficients from the received sequence. They do *not* identify the channel first and calculate the equalizer coefficients in a second step from the channel estimate and the noise correlation sequence. In the noisy case, this procedure would yield sub-optimum equalizer coefficients if the noise correlation sequence was unknown (or estimated badly). If the objective was channel *estimation* rather than equalization, a dedicated system identification algorithm such as the EigenVector approach to blind Identification (EVI) should be the preferred choice [2, 17].

Upon a precise problem statement, the "EVA solution" to blind linear equalization is briefly reviewed in section 2. In order to ensure both uniqueness and optimality of this solution (cf. requirement R1) for any channel impulse response (R2) as well as in presence of additive Gaussian noise (R3), the novel iterative algorithm (EVA) is derived in section 3. In section 4, the EVA solution is generalized to multiple output channels to obtain GenEVA which is applied to fractional tap spacing, decision-feedback, and time-variant equalization. The paper concludes with simulation results in section 5, which illustrate the performance of GenEVA.

2 Problem statement and review of the EVA solution to blind linear equalization

Assumptions: Fig. 1 shows an equivalent discrete-time baseband model of a digital communication system. The transmitted data $d(k)$ are an independent, identically distributed (i.i.d.) sequence of random variables with zero mean, variance σ_d^2, skewness[3] γ_3^d and kurtosis[3] γ_4^d. Each symbol period T, $d(k)$ takes a (possibly complex) value from a finite set. For this reason, the channel input random process clearly is non-Gaussian with a non-zero kurtosis ($\gamma_4^d \neq 0$), while its skewness vanishes ($\gamma_3^d = 0$) due to the even probability density function of typical digital modulation signals such as *Phase Shift Keying (PSK)*, *Quadrature Amplitude Modulation (QAM)* or *Amplitude Shift Keying (ASK)*.

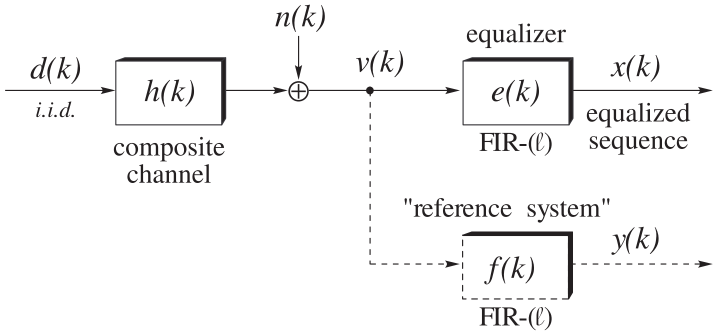

Figure 1: Equivalent symbol-rate baseband model of a digital communication system (including a linear equalizer and a "reference system")

For the composite channel, we assume the *Equivalent Discrete-Time White-Noise Filter* model [26] comprising the physical transmission channel, the transmit and receive filters, the symbol-rate sampler and the noise whitening filter. Although the composite channel is unknown, we suppose it to be time-invariant at least over a certain period of time (quasi time-invariant). It is described by the causal possibly mixed-phase impulse response $h(k)$ and will simply be termed "channel". Apart from linear distortions, the (quasi) stationary received sequence $v(k)$ is corrupted by independent stationary zero mean additive white Gaussian noise $n(k)$.

In the receiver, an FIR-(ℓ) equalizer with impulse response $e(k) = e(0), \cdots, e(\ell)$ and an FIR filter $f(k)$ of the same order are introduced. As $f(k)$ will be used to generate an implicit sequence of training (reference) data for the subsequent iteration of the iterative approach to be explained in section 3, it is termed "reference system". For now, however, assume its coefficients $f(0), \cdots, f(\ell)$ to be fixed (arbitrarily). The output sequences of the equalizer and the reference system shall be termed $x(k)$ and $y(k)$, respectively.

All signals and systems are assumed to be complex-valued due to the equivalent baseband representation of the corresponding bandpass communication system.

Linear equalization objective: Adjust the $\ell + 1$ coefficients $e(k)$ so that the equalized sequence $x(k)$ is as close as possible to the delayed transmitted data $d(k - k_0)$ in the *MSE (mean square error)* sense

$$\mathrm{MSE}(\mathbf{e}, k_0) \;\triangleq\; E\{|x(k) - d(k - k_0)|^2\} \overset{!}{=} \min \;, \tag{1}$$

[3]defined as $\gamma_3^d \triangleq E\{(d(k))^3\}$ and $\gamma_4^d \triangleq E\{|d(k)|^4\} - 2\sigma_d^4 - |E\{d^2(k)\}|^2$, where $E\{\cdot\}$ denotes statistical expectation.

where the vector $\mathbf{e} = [e(0), \cdots, e(\ell)]^T$ is used to simplify notation. For each order ℓ and delay k_0, the equalizer minimising (1) is called *Minimum Mean Square Error* equalizer[4] denoted MMSE-(ℓ, k_0).

Non-blind solution: If both the received sequence $v(k)$ and some transmitted data $d(k)$ *(training sequence)* are given, the MMSE-(ℓ, k_0) equalizer coefficients can be calculated using the well-known *normal equation* [12]

$$\mathbf{e}_{\,\mathrm{MMSE}(k_0)} = \mathbf{R}_{vv}^{-1}\,\mathbf{r}_{vd} \qquad \text{with} \qquad \begin{cases} \mathbf{r}_{vd} & \triangleq\; E\{\mathbf{v}_k \cdot d(k-k_0)\} \\ \mathbf{R}_{vv} & \triangleq\; E\{\mathbf{v}_k \mathbf{v}_k^*\} \end{cases} \tag{2}$$

where $\mathbf{r}_{vd}$ and $\mathbf{R}_{vv}$ denote the cross-correlation vector and the non-singular $(\ell+1)\times(\ell+1)$ Hermitian Toeplitz autocorrelation matrix, respectively, and the vectors $\mathbf{v}_k$ and $\mathbf{v}_k^*$ are defined as

$$\mathbf{v}_k \;\triangleq\; [v^*(k), v^*(k-1), \cdots, v^*(k-\ell)]^T \qquad \text{and} \tag{3}$$

$$\mathbf{v}_k^* \;\triangleq\; [v(k), v(k-1), \cdots, v(k-\ell)] \qquad \text{(conjugate transpose form)}\;. \tag{4}$$

The MMSE-(ℓ, k_0) equalizer $\mathbf{e}_{\,\mathrm{MMSE}(k_0)} \triangleq [e_{\,\mathrm{MMSE}}(0), \cdots, e_{\,\mathrm{MMSE}}(\ell)]^T$ according to (2) will be used as a reference in this paper. In the noiseless case, it approximates the channel's inverse system (deconvolution, *zero forcing*) in order to minimize intersymbol interference (ISI). If additive noise is present, however, its coefficients are adjusted differently so as to minimize the total MSE in the equalized sequence $x(k)$ due to ISI *and noise.*

Blind "EVA solution": With *blind* equalization, the objective is to determine the MMSE-(ℓ, k_0) equalizer coefficients *without access to the transmitted data*, i.e. from the received sequence $v(k)$ only. As both the output $x(k)$ of the equalizer and the output $y(k)$ of the reference system can be derived from $v(k)$ in the receiver, we may consider the two-dimensional fourth order cross-cumulant sequence[5]

$$\begin{aligned} c_4^{xy}(i_1, i_2) \;&\triangleq\; c_4^{xyxy}(i_1, 0, i_2) \\ &=\; E\{|x(k)|^2\, y^*(k+i_1)\, y(k+i_2)\} - r_{xx}(0)\, r_{yy}(i_2 - i_1) - r_{xy}(i_2)\, r_{xy}^*(i_1) - \bar{r}_{xy}^*(i_1)\, \bar{r}_{xy}(i_2) \end{aligned} \tag{5}$$

where $r_{xx}(i)$, $r_{xy}(i)$, and $\bar{r}_{xy}(i)$ denote the auto-correlation, the cross-correlation and the modified cross-correlation sequences, respectively,

$$r_{xx}(i) \;\triangleq\; E\{x^*(k)\, x(k+i)\}; \quad r_{xy}(i) \;\triangleq\; E\{x^*(k)\, y(k+i)\}; \quad \bar{r}_{xy}(i) \;\triangleq\; E\{x(k)\, y(k+i)\}\;. \tag{6}$$

Similar to Shalvi/Weinstein's *maximum kurtosis* criterion [30, 31], our solution to blind equalization is based on a *maximum "cross-kurtosis"* quality function. We have demonstrated in [16, sec. 3] that

$$c_4^{xy}(0,0) \;=\; E\{|x(k)|^2\, |y(k)|^2\} - E\{|x(k)|^2\}\, E\{|y(k)|^2\} - |E\{x^*(k)\, y(k)\}|^2 - |E\{x(k)\, y(k)\}|^2\,, \tag{7}$$

i.e. the cross-kurtosis between $x(k)$ and $y(k)$, can be used as a measure for equalization quality[6]:

$$\text{maximize} \quad |c_4^{xy}(0,0)| \qquad \text{subject to} \qquad r_{xx}(0) = \sigma_d^2\;. \tag{8}$$

[4] An additional optimization with respect to the delay time k_0 would deliver *the* optimum linear equalizer MMSE-(ℓ). However, as MSE$(\mathbf{e}, k_0)$ does not change much over a wide range of delays [38], we can simply let $k_0 = \lfloor \ell/2 \rfloor$.

[5] Third order cumulants can not be exploited due to the zero skewness γ_3^d of typical digital modulation signals.

[6] Similar fourth order cumulant-based criteria for blind source separation were proposed by Cardoso et al. [5, 6, 4].

Rather than referring to the equalizer output $x(k)$, this scalar quality function can easily be expressed in terms of the equalizer *input* $v(k)$ by replacing $x(k)$ in equation (7) with $x(k) = v(k) * e(k) = \mathbf{v}_k^* \mathbf{e}$, where "$*$" denotes the convolution operator. In this way, we obtain from (8)

$$\text{maximize } |\mathbf{e}^* \mathbf{C}_4^{yv} \mathbf{e}| \qquad \text{subject to} \qquad \mathbf{e}^* \mathbf{R}_{vv} \mathbf{e} = \sigma_d^2 \ , \tag{9}$$

where the Hermitian $(\ell+1) \times (\ell+1)$ cross-cumulant matrix

$$\mathbf{C}_4^{yv} \triangleq E\{|y(k)|^2 \mathbf{v}_k \mathbf{v}_k^*\} - E\{|y(k)|^2\} E\{\mathbf{v}_k \mathbf{v}_k^*\} - E\{y(k)\mathbf{v}_k\} E\{y^*(k)\mathbf{v}_k^*\} - E\{y^*(k)\mathbf{v}_k\} E\{y(k)\mathbf{v}_k^*\} \tag{10}$$

can be rewritten in terms of the scalar cross-cumulants[7] $c_4^{yv}(\cdot)$ defined according to (5)

$$\mathbf{C}_4^{yv} = \begin{bmatrix} c_4^{yv}(0,0) & [c_4^{yv}(-1,0)]^* & \cdots & [c_4^{yv}(-\ell,0)]^* \\ c_4^{yv}(-1,0) & c_4^{yv}(-1,-1) & \cdots & [c_4^{yv}(-\ell,-1)]^* \\ \vdots & \vdots & \ddots & \vdots \\ c_4^{yv}(-\ell,0) & c_4^{yv}(-\ell,-1) & \cdots & c_4^{yv}(-\ell,-\ell) \end{bmatrix} . \tag{11}$$

The quality function (9) is quadratic in the equalizer coefficients. Its optimization leads to a closed-form expression in guise of the generalized eigenvector problem [16]

$$\boxed{\mathbf{C}_4^{yv} \mathbf{e}_{\text{EVA}} = \lambda \mathbf{R}_{vv} \mathbf{e}_{\text{EVA}}} \qquad\qquad \textbf{"EVA equation"} \tag{12}$$

which we term "EVA equation". The coefficient vector $\mathbf{e}_{\text{EVA}} \triangleq [e_{\text{EVA}}(0), \cdots, e_{\text{EVA}}(\ell)]^T$ obtained by choosing the eigenvector of $\mathbf{R}_{vv}^{-1} \mathbf{C}_4^{yv}$ associated with the maximum magnitude eigenvalue λ is called the **"EVA-(ℓ) solution"** to the problem of blind equalization. Note that it can only be determined up to a complex factor from equation (12). Although the magnitude of this factor can be fixed by an automatic gain control ensuring $r_{xx}(0) = \sigma_d^2$ according to (8), its phase remains indeterminate.

Apart from this ambiguity, the EVA solution is unique if the quality function (8) has a single global maximum. In [15, 16], we have proven that this is the case if and only if the magnitude of the combined impulse response $w(k) \triangleq h(k) * f(k)$ adopts its maximum value $w_m \triangleq \max\{|w(k)|\}$ only once, i.e.

$$\left. \begin{array}{ll} |w(k)| = w_m & \text{if } k = k_m \\ |w(k)| < w_m & \text{otherwise} \end{array} \right\} \iff \text{EVA-}(\ell) \text{ solution is unique .} \tag{13}$$

Of course, condition (13) can not be guaranteed since the channel impulse response $h(k)$ and thus $w(k)$ are unknown. However, the effects of an "unlucky guess" of $f(k)$ resulting in a violation of (13) can be overcome by an iterative adjustment of the reference system's coefficients. Such an iterative algorithm will be presented in the following section.

[7] where the symmetry property $c_4^{yv}(i_1, i_2) = [c_4^{yv}(i_2, i_1)]^*$ is exploited.

3 EigenVector Algorithm for blind linear equalization (EVA)

The EVA-(ℓ) solution $\mathbf{e}_{\mathrm{EVA}}$ can be decomposed into a linear combination of MMSE-(ℓ, k) equalizers $\mathbf{e}_{\mathrm{MMSE}(k)}$ with different delay times k [16]

$$\mathbf{e}_{\mathrm{EVA}} = \frac{\gamma_4^d}{\lambda\,\sigma_d^2} \sum_k |w(k)|^2\, s(k)\, \mathbf{e}_{\mathrm{MMSE}(k)} \qquad \text{with} \quad \left\{ \begin{array}{rcl} w(k) & \triangleq & h(k) * f(k) \\ s(k) & \triangleq & h(k) * e_{\mathrm{EVA}}(k)\ , \end{array} \right. \tag{14}$$

where $\mathbf{e}_{\mathrm{MMSE}(k)}$ was defined in eq. (2). Recalling that the optimum result consists in the selection of a single MMSE-(ℓ, k_m) equalizer from the sum in (14), the following statements can be made:

(a) On ideal conditions ($\ell \to \infty$, no additive noise), perfect channel deconvolution is possible, i.e. $s(k) \propto \delta(k - k_m)$. Therefore, the optimum result $\mathbf{e}_{\mathrm{MMSE}(k_m)}$ is selected from (14) *regardless of the values of* $w(k)$ provided that the uniqueness condition (13) is met.

(b) For a finite order ℓ or in presence of additive noise, $s(k)$ no longer represents a delay. Thus, in order to select $\mathbf{e}_{\mathrm{MMSE}(k_m)}$ in (14), the reference system $f(k)$ should be chosen such that[8]

$$w(k) = w(k_m) \cdot \delta(k - k_m), \qquad \text{where} \qquad |w(k_m)| \neq 0\ . \tag{15}$$

Although (15) would obviously satisfy (13), it can not be guaranteed since $w(k)$ is unknown.

(c) In the realistic case (finite ℓ and/or additive noise, arbitrary $w(k)$ differing from (15)), a sum of MMSE-(ℓ, k) equalizers weighted by $|w(k)|^2\, s(k)$ is obtained from (14). *The quicker* $|w(k)|^2$ *decays as its index* k *departs from lag* k_m*, the closer* $\mathbf{e}_{\mathrm{EVA}}$ *will be to* $\mathbf{e}_{\mathrm{MMSE}(k_m)}$ – provided that uniqueness is ensured. For this reason, $|w(k)|$ should have *a distinct peak value*

$$|w(k_m)| \gg |w(k)| \qquad \text{for} \quad k \neq k_m\ . \tag{16}$$

The influence of $|w(k)|$ on the quality of the EVA solution is demonstrated by two simulation results (note that the main simulation parameters are summarized in Table 2). In the first example, true values of $\mathbf{R}_{vv}$ and $\mathbf{C}_4^{yv}$ are used in equation (12) to attain the "asymptotic" EVA solution, while these matrices are estimated from finite blocks of data samples in the second example. As we assume the noiseless case, equalization performance of the EVA-(ℓ) solution $e_{\mathrm{EVA}}(k)$ can be assessed by the power of residual intersymbol interference (ISI) after equalization (also see [30])

$$\mathrm{ISI}_{\mathrm{EVA}} \triangleq \frac{\sum_{k \neq k_s} |s(k)|^2}{|s(k_s)|^2} \qquad \text{with} \quad \left\{ \begin{array}{rcl} s(k) & \triangleq & h(k) * e_{\mathrm{EVA}}(k) \\ |s(k_s)| & \triangleq & \max\{|s(k)|\}\ . \end{array} \right. \tag{17}$$

Remember that for each order ℓ, the minimum value $\mathrm{ISI}_{\min}$ is obtained from (17) if the MMSE equalizer $e_{\mathrm{MMSE}}(k)$ according to equation (2) is used in place of $e_{\mathrm{EVA}}(k)$.

In Figure 2, the sensitivity of the asymptotic EVA solution[9] with respect to the uniqueness condition is investigated. As can be seen from the small subplot, we select a fourth order channel example[10] C1 (see Table 1) with two maximum magnitude coefficients $|h(1)| \equiv |h(2)|$. Using the reference system

$$f(k) = \delta(k - k_0) - f(1)\, \delta(k - k_0 - 1)\ , \tag{18}$$

[8] Remark: If equation (15) holds, $y(k)$ is proportional to $d(k - k_m)$, i.e. the matrix $\mathbf{C}_4^{yv}$ in equation (12) refers to a training sequence and EVA becomes a non-blind approach using $c_4^{xd}(0,0)$ as a quality criterion. In this case, $f(k)$ generates a sequence of reference data within the receiver. Hence its designation as "reference system".

[9] corresponding to the consistent "estimation" of $\mathbf{R}_{vv}$ and $\mathbf{C}_4^{yv}$ from sequences $v(k)$ and $y(k)$ with infinite length.

[10] Channel C1: $h(k) = -0.4j\,\delta(k) + \delta(k-1) + (-0.6 + 0.8j)\,\delta(k-2) + (0.2 - 0.5j)\,\delta(k-3) - 0.3\,\delta(k-4)$.

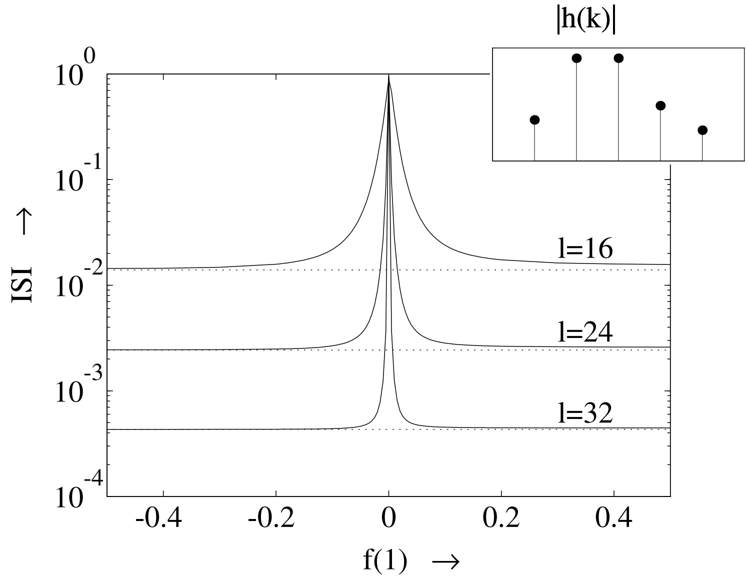

Figure 2: Sensitivity of the asymptotic EVA-(ℓ) solution to the uniqueness condition (13)
$d(k)$: QPSK; $h(k)$: C1 (two maximum magnitude coefficients)
EVA solution for: $f(1)$ varying; $L \to \infty$; $\ell = 16$, 24, and 32 (denoted l, here)

the uniqueness condition (13) can be violated deliberately by setting $f(1)$ to zero, because this results in $w(k) = h(k - k_0)$ having two peak amplitude coefficients, too. The sensitivity of the EVA-(ℓ) solution to the violation of (13) can be assessed by observing ISI for a range of values $f(1)$ around zero. The solid lines in Fig. 2 display $\mathrm{ISI}_{\mathrm{EVA}}$ according to (17) for the orders $\ell = 16$, 24, and 32 and the delay times $k_0 = \ell/2$. For comparison, the $\mathrm{ISI}_{\min}$ values are indicated by dotted lines. While they are approached to a satisfactory extent for a wide range of $f(1)$ values, it is clear that $\mathrm{ISI}_{\mathrm{EVA}}$ is increased at $f(1) = 0$ for any order ℓ. Notice that the region of $f(1)$ values where $\mathrm{ISI}_{\mathrm{EVA}}$ largely differs from $\mathrm{ISI}_{\min}$ gets smaller as ℓ is increased. According to the above statement (a), for $\ell \to \infty$, a non-zero value of $\mathrm{ISI}_{\mathrm{EVA}}$ would only occur if $f(1)$ vanished exactly.

Reconsider Fig. 1 for the explanation of the second simulation. An i.i.d. sequence $d(k)$ of *Quarternary Phase Shift Keying (QPSK)* symbols is propagated through the sixth order channel example[11] C2. Using L samples of the noiseless steady-state received sequence $v(k)$ and 3 different reference systems to obtain $y(k)$, RLS-type estimates $\widehat{\mathbf{R}}_{vv}$ and $\widehat{\mathbf{C}}_4^{yv}$ were calculated according to Appendix A and used in place of $\mathbf{R}_{vv}$ and $\mathbf{C}_4^{yv}$ in eq. (12) to determine an EVA-(ℓ) solution $e_{\mathrm{EVA},j}(k)$, $j = 1, 2, 3$ for each reference system. The three reference systems $f_j(k)$ of order $\ell = 32$ were chosen such that the combined impulse responses $w_j(k) = h(k) * f_j(k)$ shown in Figure 3a were generated: $f_1(k)$ equalizes the channel in the MMSE sense according to (2), $f_2(k)$ consists of a simple delay resulting in $w_2(k) = h(k - 15)$, and $f_3(k) = \delta(k-15) + (0.529 + 0.235j)\,\delta(k-16)$ leads to $w_3(k)$ with two max. magnitude coefficients. Figure 3b displays the deconvolution results $s_j(k) = h(k) * e_{\mathrm{EVA},j}(k)$ based on EVA-(32) solutions derived from $L = 1000$ received data samples. In accordance with statement (b), the best result is returned if equation (15) holds as closely as possible (refer to the left subplots of Fig. 3a,b). Because of a quickly decaying magnitude of $w_2(k)$, the result $s_2(k)$ is quite satisfactory, too (see statement (c)). As for $s_3(k)$, however, no equalization is possible due to the violation of (13) by $w_3(k)$.

[11] Channel C2: $h(k) = (0.8 - 0.6j)\,\delta(k) + (0.5 + 0.3j)\,\delta(k-1) + (0.2 - 0.9j)\,\delta(k-2) + (1.9 + 0.8j)\,\delta(k-3) +$
$+ (1.4 - 0.5j)\,\delta(k-4) + 1.1\,\delta(k-5) + (0.7 + 0.5j)\,\delta(k-6)$.

a) Three different magnitude impulse resonses $|w_j(k)|$

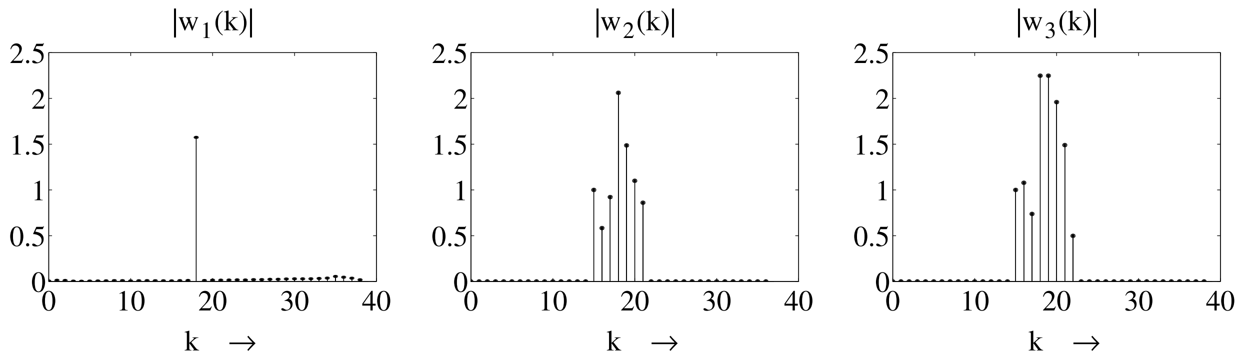

b) Deconvolution results $|s_j(k)|$ from $L = 1000$ received data samples

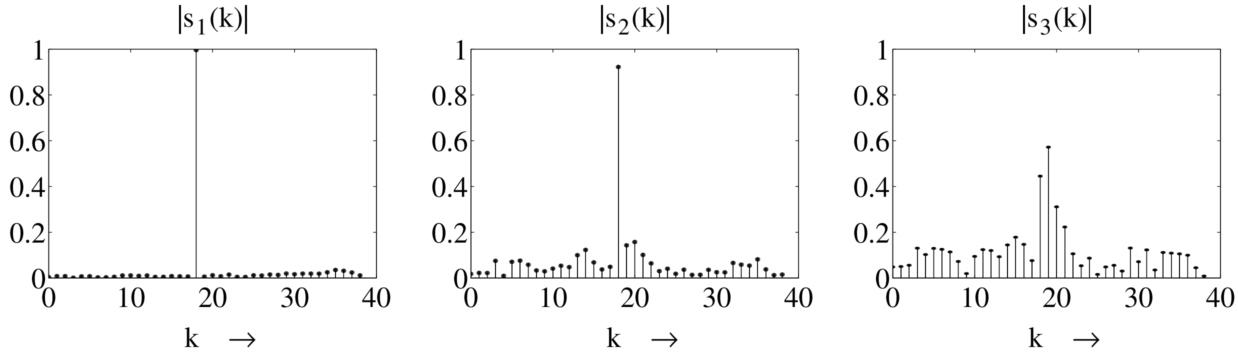

c) Convergence behavior for $w_1(k)$, $w_2(k)$, and $w_3(k)$

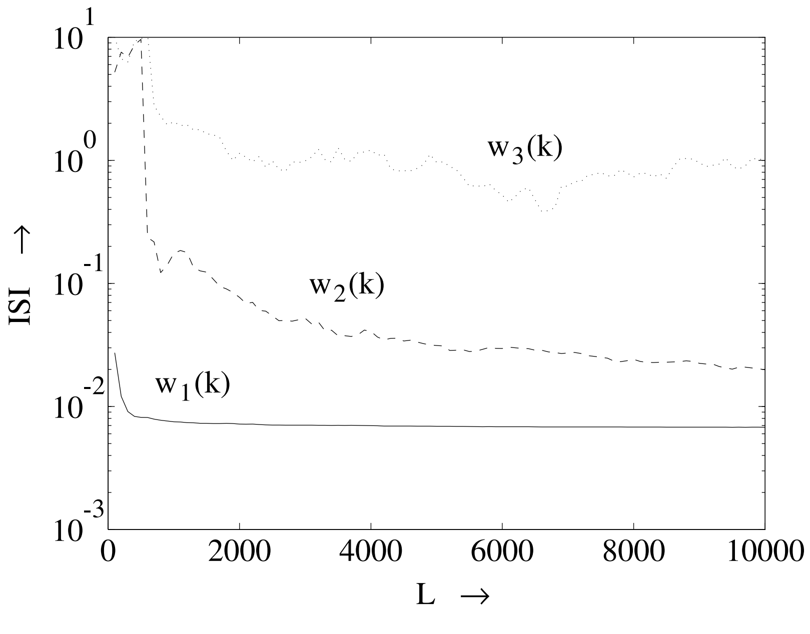

Figure 3: Influence of $w(k)$ on the quality and convergence rate of the EVA-(32) solution
$d(k)$: QPSK; $h(k)$: C2 (a single maximum magnitude coefficient)
EVA solution for: three ref. systems; $L = 1000$ (Fig. b) and varying (Fig. c); $\ell = 32$

Fig. 3c illustrates the influence of $|w(k)|$ on the *convergence rate* of the EVA solution, i.e. on the decay rate of $\mathrm{ISI}_{\mathrm{EVA}}$ as the number L of received data samples used to estimate $\mathbf{R}_{vv}$ and $\mathbf{C}_4^{yv}$ is increased. The observations made for $L = 1000$ samples (Fig. 3b) remain valid for other blocklengths L. Furthermore, we realize that *the more dominant the peak value of $|w(k)|$ is, the higher the convergence rate will be.*

In other words: The better the reference system deconvolves the channel (see eq. (15) and (16)), the better the resulting EVA solution will be. For this reason, an iterative procedure to adjust the reference system's coefficients was suggested where $f(k)$ *is loaded with the equalizer impulse response calculated in the previous iteration* [15]. After some iterations (based on the same block of received data samples), both the reference system and the equalizer will have the same impulse response being very close to the MMSE-(ℓ, k_m) equalizer. This iterative algorithm, termed EVA standing for EIGENVECTOR ALGORITHM FOR BLIND EQUALIZATION, comprises the following steps (note that a superscript index in parenthesis (as in $f^{(i)}(k)$, for instance) indicates an iterative update):

EIGENVECTOR ALGORITHM FOR BLIND LINEAR EQUALIZATION (EVA)[a]:

S0: Set the reference system to $f^{(0)}(k) = \delta(k - \lfloor \ell/2 \rfloor)$ and the iteration counter to $i = 0$. From $v(0), \cdots, v(L-1)$, estimate the $(\ell+1) \times (\ell+1)$ matrix $\mathbf{R}_{vv} \Rightarrow \widehat{\mathbf{R}}_{vv}$.
S1: Determine $y(k) = v(k) * f^{(i)}(k)$ and estimate the $(\ell+1) \times (\ell+1)$ matrix $\mathbf{C}_4^{yv} \Rightarrow \widehat{\mathbf{C}}_4^{yv}$.
S2: With $\widehat{\mathbf{R}}_{vv}$ and $\widehat{\mathbf{C}}_4^{yv}$ substituted for $\mathbf{R}_{vv}$ and $\mathbf{C}_4^{yv}$ in equation (12), calculate the "EVA-(ℓ) solution" $\mathbf{e}_{\mathrm{EVA}}$ by choosing the most significant eigenvector of $\widehat{\mathbf{R}}_{vv}^{-1}\widehat{\mathbf{C}}_4^{yv}$. Let $e_{\mathrm{EVA}}^{(i)}(k)$ denote the equalizer coefficients associated with $\mathbf{e}_{\mathrm{EVA}}$.
S3: Load $e_{\mathrm{EVA}}^{(i)}(k)$ into the reference system, i.e. let $f^{(i+1)}(k) = e_{\mathrm{EVA}}^{(i)}(k)$. Increment the iteration counter: $i \to i+1$; if $i < \mathcal{I}$ goto step S1.

[a]Parameters: L, ℓ, $\mathcal{I}$; input: $v(0), \cdots, v(L-1)$.

Considering this iteration we observe that the idea of a "reference system" is not really necessary: If we replace $f^{(i+1)}(k)$ with $e_{\mathrm{EVA}}^{(i)}(k)$ we see that the algorithm explained above just describes an *iterative update of the equalizer impulse response*.

The convergence behavior of EVA is demonstrated in Figure 4 by a simulation result based on a QPSK transmission over the channel C1 (see footnote 10). $L = 500$ samples of $v(k)$ are used to determine the $(\ell+1) \times (\ell+1)$ matrices $\widehat{\mathbf{R}}_{vv}$ and $\widehat{\mathbf{C}}_4^{yv}$ for $\ell = 32$ (see Appendix A). Figure 4 illustrates the updating process where the initial reference system is set to $f^{(0)}(k) = \delta(k-16)$ so that the initial combined impulse response $w^{(0)}(k) = h(k) * f^{(0)}(k)$ contains two maximum magnitude coefficients (see Fig. 4a). Obviously, this example is particularly unfavorable due to the violation of (13) by $w^{(0)}(k)$. Therefore, the EVA-(32) solution $e_{\mathrm{EVA}}^{(0)}(k)$ achieved in step S2 does not yet deconvolve the channel sufficiently, as can be seen from Fig. 4b, which displays the magnitude of $s^{(0)}(k) = h(k) * e_{\mathrm{EVA}}^{(0)}(k)$. However, loading $e_{\mathrm{EVA}}^{(0)}(k)$ into $f^{(1)}(k)$ in step S3 to obtain $w^{(1)}(k) = h(k) * f^{(1)}(k) \equiv s^{(0)}(k)$, we realize that (13) is satisfied, now. Thus, the second iteration of EVA delivers a better equalizer $e_{\mathrm{EVA}}^{(1)}(k)$ leading to $s^{(1)}(k) = h(k) * e_{\mathrm{EVA}}^{(1)}(k)$ which is shown in Fig. 4c. A relatively good equalization quality is achieved after the third iteration (see Fig. 4d). From this example, we can state that *an initial violation of (13) does not affect the (final) equalization quality*, i.e. the convergence rate (defined *in terms of* L). It just slows down convergence *in terms of* i so that an increased number $\mathcal{I}$ of EVA iterations is required. As the same block of received data samples is used for all iterations i, this is just a matter of computational effort rather than a question of equalization quality obtainable from a finite number of samples.

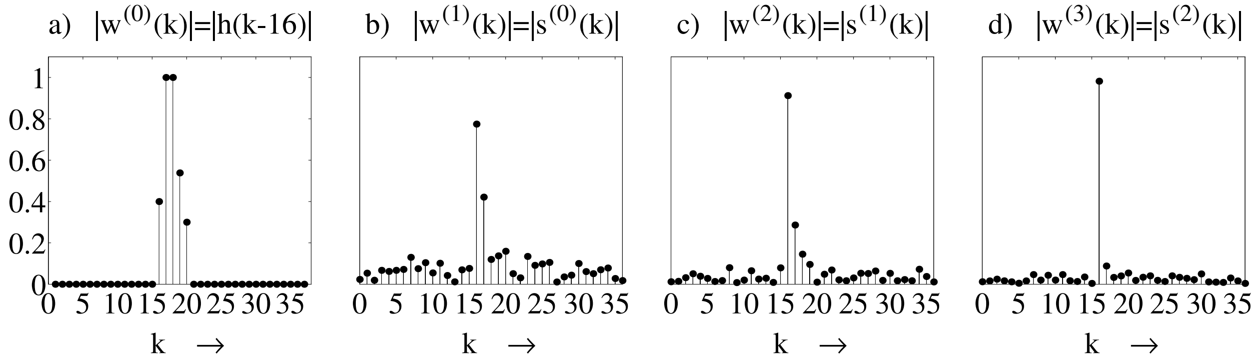

Figure 4: Iterative adjustment of the reference system and the equalizer by EVA
$d(k)$: QPSK; $h(k)$: C1 (two maximum magnitude coefficients)
EVA parameters: $L = 500$; $\ell = 32$; $\mathcal{I} = 3$

Let us introduce a small modification to the iteration process. Evidently, the convergence rate strongly depends on the number of parameters to be updated, i.e. the order ℓ of the equalizer. Since for the initial iterations, the goal simply is the generation of an impulse response $w(k)$ which satisfies (13) and roughly approximates (16), it is convenient to perform a *stepwise increase of the equalizer order* (as suggested in [37], e.g.). Therefore, we start with a rather small order $\ell^{(0)} < \ell$ of the reference system $f^{(0)}(k)$, execute $\mathcal{I}^{(0)}$ EVA iterations according to the scheme described above, increase the order to $\ell^{(1)} < \ell$ by prepending and appending $\ell^{(1)} - \ell^{(0)}$ zeros to the reference system in step S3, execute further $\mathcal{I}^{(1)}$ iterations, and finally, terminate with $\mathcal{I}^{(N-1)}$ iterations based on $\ell^{(N-1)} = \ell$. Comparing this with $\mathcal{I} = \sum \mathcal{I}^{(\xi)}$ iterations for a fixed order $\ell^{(N-1)}$, a considerable improvement in convergence is attained. In the remainder of the paper, "EVA" implies the overall algorithm including the stepwise order increase.

Thus, the parameters of EVA are:

L:	Number of received data samples $v(0), \cdots, v(L-1)$ used to calculate $\widehat{\mathbf{R}}_{vv}$ and $\widehat{\mathbf{C}}_4^{yv}$ according to Appendix A.
$\boldsymbol{\ell} \triangleq [\ell^{(0)}, \cdots, \ell^{(N-1)}]$:	The orders of the equalizer and the reference system, where $\ell^{(0)} < \ell^{(1)} < \cdots < \ell^{(N-1)}$.
$\boldsymbol{i} \triangleq [\mathcal{I}^{(0)}, \cdots, \mathcal{I}^{(N-1)}]$:	Numbers of EVA iterations executed for each order $\ell^{(\xi)}$.

For the modulation scheme and the channel used for Fig. 4, the convergence rates of three equalization algorithms can be seen in Figure 5, where ISI is displayed in terms of the number L of samples $v(k)$ used to adjust the coefficients of the FIR-(32) equalizer. The solid line refers to the RECURSIVE LEAST SQUARES (RLS) algorithm with unit forgetting factor. It exhibits a brilliant convergence rate leading to ISI values inferior to 10^{-3} for as few as $L = 80$ received samples. As the correlation coefficients can *not* be estimated with sufficient precision from 80 samples, this is due to the relative robustness

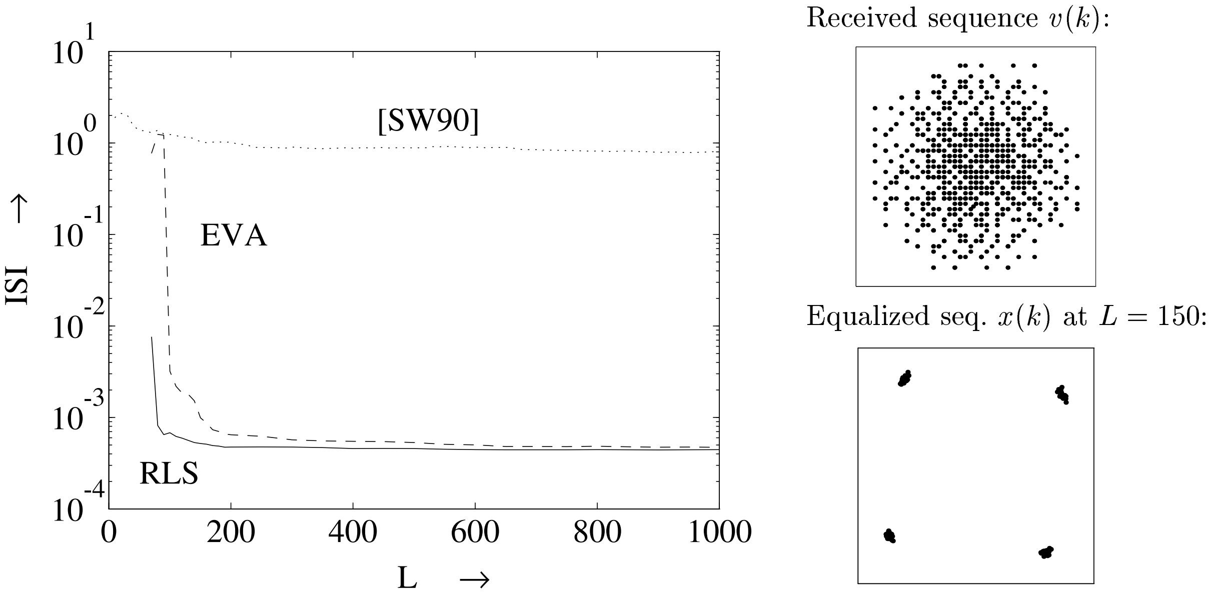

Figure 5: Convergence rate of three equalization approaches for QPSK
$d(k)$: QPSK; $h(k)$: C1 (two maximum magnitude coefficients)
EVA parameters: L varying; $\boldsymbol{\ell} = [4, 8, 16, 32]$; $\boldsymbol{i} = [10, 10, 10, 10]$
RLS parameters: L varying; $\ell = 32$; forgetting factor $= 1$

of RLS with respect to errors in the correlation estimates. Appendix B gives a reasoning for this robustness. Now, consider the dashed line in Fig. 4, where $\mathcal{I}^{(\xi)} = 10$ EVA iterations are executed for each order in $\boldsymbol{\ell} = [4, 8, 16, 32]$ and the initial reference system is set to $f^{(0)}(k) = \delta(k-2)$. It turns out that for $L > 140$, *EVA closely approaches the convergence performance of RLS*. This needs to be emphasized because *(i)* RLS falls into the category of non-blind methods and *(ii)* we have chosen the channel C1 which is unfavorable for EVA (as it requires high values of $\mathcal{I}^{(\xi)}$). Bearing in mind that EVA uses fourth order cumulants, it is obvious that they can *not* be estimated satisfactorily from 140 samples. Similar to RLS, *EVA is robust with respect to errors in the correlation and cumulant estimates*, because they cancel each other, to some extent, in the EVA equation (12), as we justify in Appendix C. This is fundamental in understanding EVA's performance based on small sample sizes. As a 3rd approach, the blind algorithm [SW90] published by Shalvi and Weinstein [30] is considered. It is based on a simple stochastic gradient search, where we have optimized the stepsize parameter for convergence speed rather than final equalization quality (leading to a non-negligible gradient noise). From the dotted line, we realize that the convergence rate of [SW90] is clearly[12] inferior to that of EVA or RLS.

While the upper small subplot in Fig. 5 displays the original received sequence $v(k)$ in the complex plane, the bottom one shows the equalized data $x(k)$ obtained with EVA from as few as $L = 150$ samples. Equalization of the QPSK signal is achieved up to a complex factor.

[12]We have demonstrated in [14] that some performance gain can be obtained over [SW90] by using a lattice prewhitening filter followed by a cascade of 1st order allpass systems. However, we could in no way approximate RLS' performance as closely as EVA does. As such equalizer structures suffer from several principal disadvantages (such as the additional time the prewhitening filter requires for convergence and the suboptimum solution in presence of additive Gaussian noise), we did not consider advanced (block) gradient methods although further improvements appear likely.

We conclude this section with a simulation result based on 16-ary Quadrature Amplitude Modulation (16-QAM). The channel impulse response and the EVA parameters are chosen in accordance with those used for Figure 5. For the reasons stated in Appendix D, the convergence rate decreases for amplitude modulated signals [13, 15]. This can be seen from Figure 6, where the equalized sequence $x(k)$ is shown in the complex plane for $L = 300$ (left subplot), 500 and 1000 (right) samples of the received sequence $v(k)$. For a secure decision, we would require about 1000 samples of the received signal in this example. Remembering that EVA represents an approach based on HOS and we have selected a channel with two maximum magnitude coefficients, this result still appears to be acceptable.

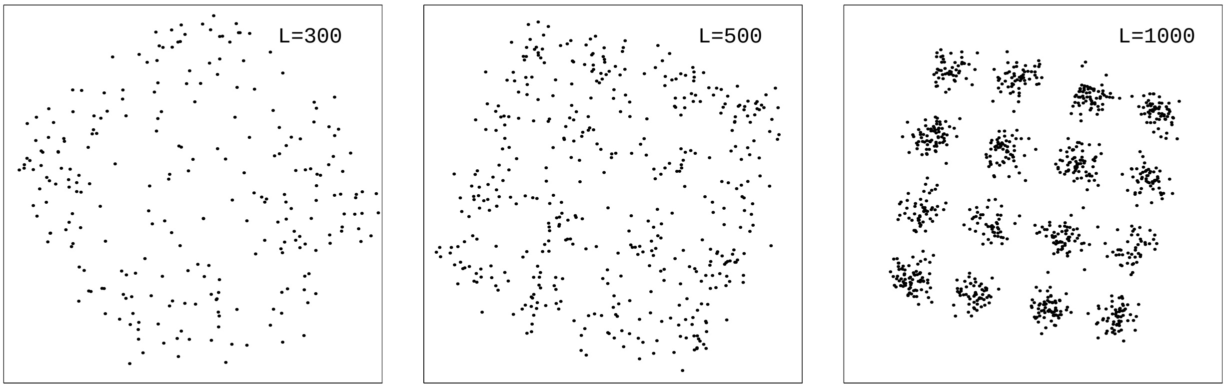

Figure 6: EVA convergence rate for an amplitude modulated signal
$d(k)$: 16-QAM; $h(k)$: C1 (two maximum magnitude coefficients)
EVA par.: $L = 300, 500, 1000$; $\boldsymbol{\ell} = [4, 8, 16, 32]$; $\boldsymbol{i} = [10, 10, 10, 10]$

In 1993, Shalvi and Weinstein [31] published an algorithm for blind equalization which converges approximately as fast as EVA. This can be explained by the fact that EVA becomes very similar to their approach if the eigenvector calculation in equation (12) is replaced with the Power Method [11]. Thus, [31] turns out to be a special case of EVA where a particular numerical method is applied to calculate the eigenvectors (note that [31] can be derived from EVA, but not vice-versa). Having stated this, it is evident that [31] also suffers from a reduced convergence rate for amplitude modulated signals.

Another blind algorithm frequently used in the field of geophysics was published by Walden in 1985 [36]. It is based on the RLS where the cross-correlation is replaced with a 4th order cross-cumulant $c_4^{xxxv}(\cdot)$. It is interesting to note that this algorithm is identical with the Shalvi/Weinstein method [31].

4 Generalization of EVA and application to fractional tap spacing, non-linear decision-feedback, and time-variant equalization

Consider the extended baseband model of a digital communication system in Figure 7. As opposed to Fig. 1, the channel is a *single input multiple output (SIMO)* system composed of M parallel subchannels $h_0(k), \cdots, h_{M-1}(k)$. Consequently, the equalizer and the reference system are also split into M subsystems $e_0(k), \cdots, e_{M-1}(k)$ and $f_0(k), \cdots, f_{M-1}(k)$ with orders $\ell_0, \cdots, \ell_{M-1}$. Let $\tilde{\ell}+1$ denote the total number of equalizer coefficients, i.e. $\tilde{\ell}+1 \triangleq \sum_{\nu=0}^{M-1}(\ell_\nu+1) = M + \sum_\nu \ell_\nu$. Notice that additive noise is suppressed in Figure 7 to enhance clarity of presentation.

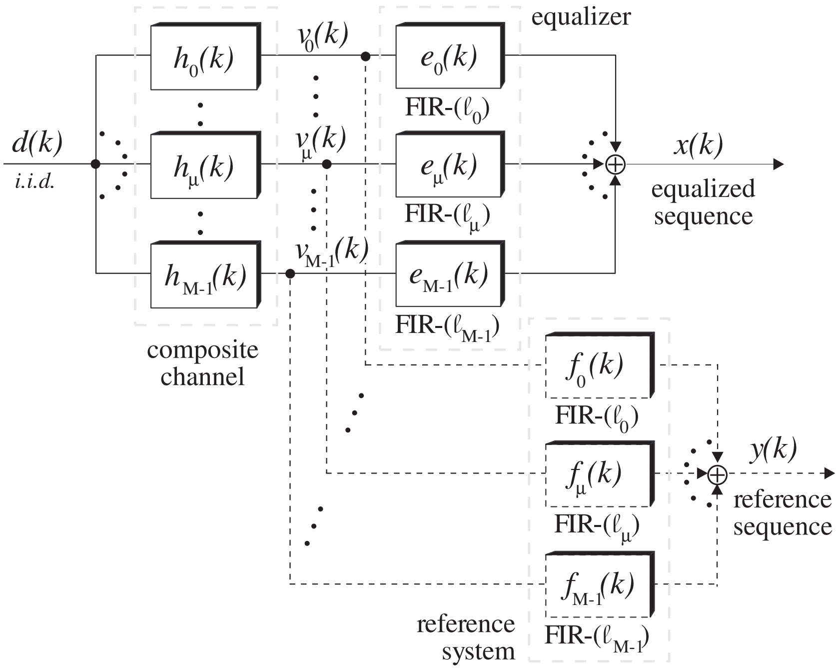

Figure 7: Extended symbol-rate model of a digital communication system with SIMO channel

For instance, the SIMO channel model can be applied directly to mobile communication systems, where the receiver has multiple antennae. Hence, we generalize in section 4.1 the EVA equation (12) to this model. In sections 4.2 to 4.4, we demonstrate that it is also suitable for the description of alternative equalizers, such as fractional tap spacing, decision-feedback, and time-variant equalizers.

4.1 EVA solution for single input multiple output channels

Let $s(k)$ and $w(k)$ denote the overall systems with input $d(k)$ and outputs $x(k)$ and $y(k)$, respectively:

$$s(k) = \sum_{\mu=0}^{M-1} h_\mu(k) * e_\mu(k) \qquad \text{and} \qquad w(k) = \sum_{\mu=0}^{M-1} h_\mu(k) * f_\mu(k)\,. \tag{19}$$

Independent from the structure of these linear (and time-invariant) systems, the cross-kurtosis remains a viable measure for equalization, so that the quality function (8) applies to Fig. 7, too. Analogous to the derivation in sec. 2, $x(k)$ in (8) can be expressed in terms of the equalizer input sequences $v_\mu(k)$

$$x(k) = \sum_{\mu=0}^{M-1} v_\mu(k) * e_\mu(k) = \tilde{\mathbf{v}}_k^* \,\tilde{\mathbf{e}}\,, \tag{20}$$

where the vectors $\tilde{\mathbf{v}}_k$ and $\tilde{\mathbf{e}}$ (length: $\tilde{\ell}+1$) are composed of M subvectors:

$$\begin{array}{lllll} \tilde{\mathbf{v}}_k^* & \stackrel{\Delta}{=} & [\mathbf{v}_{k,0}^*,\, \mathbf{v}_{k,1}^*,\, \cdots,\, \mathbf{v}_{k,M-1}^*] \quad \text{with} \quad \mathbf{v}_{k,\mu}^* & \stackrel{\Delta}{=} & [v_\mu(k), \cdots, v_\mu(k-\ell_\mu)] \\ \tilde{\mathbf{e}} & \stackrel{\Delta}{=} & [\mathbf{e}_0^T,\, \mathbf{e}_1^T,\, \cdots,\, \mathbf{e}_{M-1}^T]^T \quad \text{with} \quad \mathbf{e}_\mu & \stackrel{\Delta}{=} & [e_\mu(0), \cdots, e_\mu(\ell_\mu)]^T\;. \end{array} \tag{21}$$

Substituting $\tilde{\mathbf{v}}_k^* \,\tilde{\mathbf{e}}$ for $x(k)$ according to (20), we obtain from (8)

$$\text{maximize } |\tilde{\mathbf{e}}^* \widetilde{\mathbf{C}}_4^{yv} \tilde{\mathbf{e}}| \qquad \text{subject to} \qquad \tilde{\mathbf{e}}^* \widetilde{\mathbf{R}}_{vv} \tilde{\mathbf{e}} = \sigma_d^2\;, \tag{22}$$

where the modified $(\tilde{\ell}+1) \times (\tilde{\ell}+1)$ matrices

$$\widetilde{\mathbf{C}}_4^{yv} \stackrel{\Delta}{=} E\{|y(k)|^2 \tilde{\mathbf{v}}_k \tilde{\mathbf{v}}_k^*\} - E\{|y(k)|^2\} E\{\tilde{\mathbf{v}}_k \tilde{\mathbf{v}}_k^*\} - E\{y(k) \tilde{\mathbf{v}}_k\} E\{y^*(k) \tilde{\mathbf{v}}_k^*\} - E\{y^*(k) \tilde{\mathbf{v}}_k\} E\{y(k) \tilde{\mathbf{v}}_k^*\} \tag{23}$$

and $\widetilde{\mathbf{R}}_{vv} \stackrel{\Delta}{=} E\{\tilde{\mathbf{v}}_k \tilde{\mathbf{v}}_k^*\}$ are block Hermitian and block Toeplitz, respectively. Note that the latter matrix structure is of particular importance in multichannel processing (see [28], e.g.).

Just as in section 2, optimization of (22) leads to a generalized eigenvector problem

$$\boxed{\widetilde{\mathbf{C}}_4^{yv} \tilde{\mathbf{e}}_{\text{EVA}} = \lambda \widetilde{\mathbf{R}}_{vv} \tilde{\mathbf{e}}_{\text{EVA}}} \qquad \textbf{“GenEVA equation”} \tag{24}$$

With “Gen” standing for “generalized”, equation (24) is termed “GenEVA equation”. The coefficient vector $\tilde{\mathbf{e}}_{\text{EVA}} \stackrel{\Delta}{=} [\mathbf{e}_{\text{EVA},0}^T, \cdots, \mathbf{e}_{\text{EVA},M-1}^T]^T$ obtained by choosing the most significant eigenvector is called the **“GenEVA-($\tilde{\ell}$) solution”** to the problem of blind SIMO equalization. It is composed of M subequalizer coefficient vectors $\mathbf{e}_{\text{EVA},\mu} \stackrel{\Delta}{=} [e_{\text{EVA},\mu}(0), \cdots, e_{\text{EVA},\mu}(\ell_\mu)]^T$, where $\mu = 0, \cdots, M-1$.

With $\widetilde{\mathbf{R}}_{vv}$, $\widetilde{\mathbf{C}}_4^{yv}$, $\tilde{\mathbf{e}}_{\text{EVA}}$ used in place of $\mathbf{R}_{vv}$, $\mathbf{C}_4^{yv}$, $\mathbf{e}_{\text{EVA}}$, respectively, an iterative algorithm based on (24) can easily be derived along the lines of section 3. It is termed GENEVA and also incorporates a stepwise order increase, where the order ℓ_μ of each subsystem $f_\mu(k)$ and $e_\mu(k)$ is raised from the initial value $\ell_\mu^{(0)}$ to $\ell_\mu^{(N-1)}$. With the following description of the steps of GENEVA, $f_\mu^{(i)}(k)$ denotes the i^{th} iteration of the μ^{th} reference subsystem for a given (fixed) order $\ell_\mu^{(\xi)}$.

Generalized EigenVector Algorithm for blind equalization (GenEVA)[a]:

S0: Set the reference subsystems to $f_\mu^{(0)}(k) = \delta(k - \lfloor \ell_\mu^{(0)}/2 \rfloor)$ for $\mu = 0, \cdots, M-1$.
Set $\xi = 0$ (used to count the different orders with the stepwise order increase).

S1: Let $\tilde{\ell}^{(\xi)} \triangleq M - 1 + \sum_\mu \ell_\mu^{(\xi)}$. From $v_\mu(0), \cdots, v_\mu(L-1)$ for $\forall \mu$, estimate the $(\tilde{\ell}^{(\xi)}+1) \times (\tilde{\ell}^{(\xi)}+1)$ matrix $\widetilde{\mathbf{R}}_{vv} = E\{\tilde{\mathbf{v}}_k \tilde{\mathbf{v}}_k^*\}$. Set the iteration counter to $i = 0$.

S2: From $v_\mu(0), \cdots, v_\mu(L-1)$, $\forall \mu$, determine $y(k) = \sum_\mu v_\mu(k) * f_\mu^{(i)}(k)$ and estimate $\widetilde{\mathbf{C}}_4^{yv}$ according to (23). With the estimates of $\widetilde{\mathbf{R}}_{vv}$ and $\widetilde{\mathbf{C}}_4^{yv}$ used in (24), calculate the "GenEVA-($\tilde{\ell}^{(\xi)}$) solution" $\tilde{\mathbf{e}}_{\mathrm{EVA}}$ by choosing the most significant eigenvector.
Let $e_{\mathrm{EVA},\mu}^{(i)}(k)$ denote the subequalizer coefficients associated with $\mathbf{e}_{\mathrm{EVA},\mu}$.

S3: Load $e_{\mathrm{EVA},\mu}^{(i)}(k)$ into the reference subsystem, i.e. let $f_\mu^{(i+1)}(k) = e_{\mathrm{EVA},\mu}^{(i)}(k)$, $\forall \mu$.
Increment the iteration counter: $i \to i+1$.
If $i < \mathcal{I}^{(\xi)}$: goto step S2.
If $i = \mathcal{I}^{(\xi)}$: $\xi \to \xi + 1$;
if $\xi < N$: prepend and append $\ell_\mu^{(\xi)} - \ell_\mu^{(\xi-1)}$ zeros to $f_\mu^{(i)}(k)$;
let $f_\mu^{(0)}(k)$ denote the resulting impulse response; goto S1.

[a] Par.: M, L, $\boldsymbol{\ell}_\mu \triangleq [\ell_\mu^{(0)}, \cdots, \ell_\mu^{(N-1)}]$, $\boldsymbol{i} \triangleq [\mathcal{I}^{(0)}, \cdots, \mathcal{I}^{(N-1)}]$; input: $v_\mu(0), \cdots, v_\mu(L-1)$ for $\mu = 0, \cdots, M-1$.

4.2 Fractional tap spacing equalizer

The advantageous properties of *Fractional Tap Spacing (FTS)* equalizers have been widely discussed in literature, e.g. their capability to perfectly equalize channels with zeros on the z-plane's unit circle[13] or the weak dependence of the equalization result on the sampling phase [35].

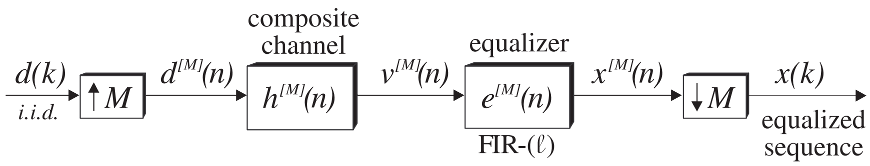

Figure 8: Communication system model with fractional tap spacing (FTS) equalizer

Figure 8 shows an FTS equalizer, where the symbols $\boxed{\uparrow M}$ and $\boxed{\downarrow M}$ describe upsampling and downsampling, respectively, by a factor of $M > 1$. The time index k refers to symbol-rate sampling while n together with a superscript $[M]$ indicates a sequence sampled at M times the symbol rate.

The received sequence $v^{[M]}(n)$ is *cyclostationary*. As the EVA equation (12) is based on a stationary sequence $v(k)$, it can *not* be applied to $v^{[M]}(n)$. However, the equalized sequence $x(k)$ can be decomposed into a sum of M sequences $x_\mu(k) = v_\mu(k) * e_\mu(k)$

$$x(k) = v^{[M]}(n) * e^{[M]}(n)\Big|_{n=kM} = \sum_\nu e^{[M]}(\nu)\, v^{[M]}(kM - \nu) \,, \qquad \text{let} \quad \nu = \eta M + \mu$$

[13] which is impossible for symbol-rate FIR equalizers with finite order.

$$= \sum_{\mu=0}^{M-1} \sum_{\eta} e^{[M]}(\eta M + \mu)\, v^{[M]}((k-\eta)M - \mu) = \sum_{\mu=0}^{M-1} \sum_{\eta} e_\mu(\eta)\, v_\mu(k-\eta) = \sum_{\mu=0}^{M-1} e_\mu(k) * v_\mu(k) \quad (25)$$

where $e_\mu(k) \triangleq e^{[M]}(kM+\mu)$ and $v_\mu(k) \triangleq v^{[M]}(kM-\mu)$ denote the μ^{th} polyphase components of $e^{[M]}(n)$ and $v^{[M]}(n)$, respectively. According to Gardner's *Time Series Representation* [9], $v_\mu(k)$ emerges from $d(k)$ by linear filtering with the μ-th *polyphase subchannel* $h_\mu(k)$ and is therefore stationary:

$$v_\mu(k) = d(k) * h_\mu(k) \qquad \text{with} \qquad h_\mu(k) \triangleq h^{[M]}(kM+\mu)\ . \quad (26)$$

Decomposing the FTS equalizer in Fig. 8 according to equations (25) and (26), we obtain the extended model in Fig. 7 so that GenEVA can be applied directly to $v_0(k), \cdots, v_{M-1}(k)$. From the final GenEVA solution $\tilde{\mathbf{e}}_{\text{EVA}}$, the FTS equalizer impulse response $e^{[M]}(n)$ can be constructed by interleaving the stacked polyphase components $\mathbf{e}_{\text{EVA},\mu}$. This version of GenEVA is denoted FTS-EVA.

A general form of FTS is obtained when downsampling by a factor of $M_1 < M$ is performed at the equalizer input. In this case, M samples are taken within M_1 symbol periods. As the SIMO model in Figure 7 can be shown to describe such an equalization structure, GenEVA can be applied.

4.3 Decision-feedback equalizer

Consider the *Decision-Feedback (DF)* equalizer given in Figure 9a [26, 27]. It comprises a feedforward equalizer with coefficients $e_f(0), \cdots, e_f(\ell_f)$, a feedback equalizer $e_b(1), \cdots, e_b(\ell_b)$, and a decision device. Note that due to the latter component, this equalizer structure is non-linear.
Figure 9a can be redrawn according to the upper part of Fig. 9b. Adding two reference systems $f_0(k)$ and $f_1(k)$, and ignoring for a start, the problem of false decisions, i.e. assuming $\hat{d}(k) \equiv d(k)$, we realize from Figure 9b that the DF-structure represents a special case of Figure 7, where $M = 2$ and

$$\begin{array}{lllllllllllll} h_0(k) &=& h(k) & & v_0(k) &=& v(k) & & e_0(k) &=& e_f(k) & & \ell_0 = \ell_f \\ h_1(k) &=& \delta(k-k_0-1) & & v_1(k) &=& d(k-k_0-1) & & e_1(k) &=& e_b(k) & & \ell_1 = \ell_b\ . \end{array} \quad (27)$$

Using the vector

$$\tilde{\mathbf{v}}_k^* = [\mathbf{v}_{k,0}^*, \mathbf{v}_{k,1}^*] = [v(k), \cdots, v(k-\ell_f),\ d(k-k_0-1), \cdots, d(k-k_0-\ell_b)] \quad (28)$$

to determine the $(\ell_f + \ell_b + 1) \times (\ell_f + \ell_b + 1)$ matrices $\widetilde{\mathbf{C}}_4^{yv}$ and $\widetilde{\mathbf{R}}_{vv}$, the GenEVA equation (24) can therefore be applied to the DF-structure to obtain the $\ell_f + \ell_b + 1$ equalizer coefficients

$$\tilde{\mathbf{e}}_{\text{EVA}} = [\mathbf{e}_0^T, \mathbf{e}_1^T]^T = [e_f(0), \cdots, e_f(\ell_f),\ e_b(1), \cdots, e_b(\ell_b)]^T\ . \quad (29)$$

However, this requires a sufficiently well equalized and decided received sequence $\hat{d}(k)$ to be used in place of $d(k)$ in equation (28). This apparent contradiction can be solved by an iterative procedure: In a first step, linear equalization is performed by EVA according to section 3 with an increased equalizer order $\max\{\boldsymbol{\ell}\} > \ell_f$. Then, non-linear equalization is achieved in a second step with the above DF-structure. The resulting overall algorithm will be referred to as DF-EVA:

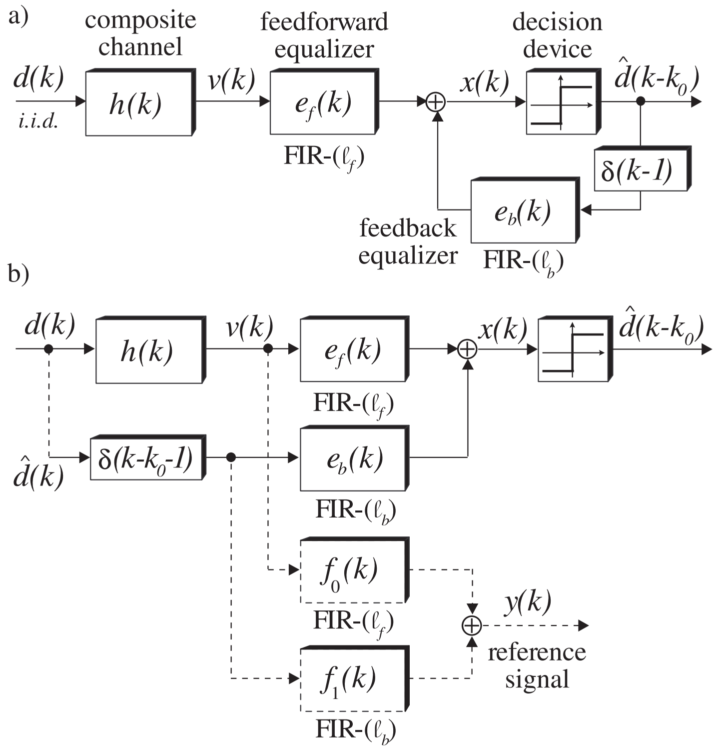

Figure 9: Communication system model with decision-feedback (DF) equalizer
a) Original structure (with a minus sign absorbed into $e_b(k)$)
b) Original structure redrawn with parallel systems

DECISION-FEEDBACK EIGENVECTOR APPROACH TO BLIND EQUALIZATION (DF-EVA)[a]:

S1: Linear EVA equalization according to section 3 $\Rightarrow$ $e_f(0), \cdots, e_f(\max\{\boldsymbol{\ell}\})$.
Tentative decision of the equalized data $x(k) = v(k) * e_f(k)$ $\Rightarrow$ $\hat{d}^{(0)}(k-k_0)$.
Reduce the order of the forward equalizer to ℓ_f and introduce the reference system $f_1(k)$ with order ℓ_b. Set the iteration counter to $i = 0$.

S2: Using (27) and (28) with $\hat{d}^{(i)}(k)$ substituted for $d(k)$, execute S1–S3 of GENEVA without stepwise order increase ($N = 1$). Once the GenEVA-($\ell_f + \ell_b$) solution $\tilde{\mathbf{e}}_{\mathrm{EVA}}$ (according to (29)) is obtained, decide $x(k) = \tilde{\mathbf{v}}_k^* \tilde{\mathbf{e}}_{\mathrm{EVA}}$ again $\Rightarrow \hat{d}^{(i+1)}(k-k_0)$, increment i, and execute another iteration of GENEVA if $i < \mathcal{I}$.

[a]Parameters: S1: L, $\boldsymbol{\ell}$, $\boldsymbol{i} = [\mathcal{I}^{(0)}, \cdots, \mathcal{I}^{(N-1)}]$, S2: ℓ_f, ℓ_b, $\mathcal{I}$; input: $v(0), \cdots, v(L-1)$.

Obviously, false decisions represent a principal problem with the derivation of DF-EVA. In step S1, an estimate $\hat{d}^{(0)}(k)$ of the original data sequence is determined by means of a symbol-rate FIR equalizer. On account of imperfect equalization and a possibly high SNR loss due to *linear* equalization, we may get a rather poor initial error rate influencing step S2. One could argue that after step S1, the problem is no longer blind, so that GENEVA in S2 could be replaced with the *DF-MMSE solution* [22]

$$\tilde{\mathbf{e}}_{\mathrm{DF}(k_0)} = \widetilde{\mathbf{R}}_{vv}^{-1}\,\tilde{\mathbf{r}}_{vd} \qquad \text{with} \qquad \begin{cases} \tilde{\mathbf{r}}_{vd} \triangleq E\{\tilde{\mathbf{v}}_k \cdot d(k-k_0)\} \\ \widetilde{\mathbf{R}}_{vv} \triangleq E\{\tilde{\mathbf{v}}_k \tilde{\mathbf{v}}_k^*\} \end{cases} \tag{30}$$

where $\tilde{\mathbf{e}}_{\mathrm{DF}(k_0)}$ is defined just as $\tilde{\mathbf{e}}_{\mathrm{EVA}}$ in (29). However, the performance of the DF-MMSE solution based on $\hat{d}^{(0)}(k)$ strongly depends on the initial error rate while DF-EVA iteratively improves the error rate. An example discussed in section 5 will demonstrate that DF-EVA converges properly even with decision errors. A result near the optimum can be obtained even *without S1*, if L is increased (which is not possible with the DF-MMSE solution). Thus, DF-EVA turns out to be robust.

It should be mentioned that the decision-feedback equalization structure can also be combined with various forms of fractional tap spacing in the forward branch. GENEVA can always be applied as long as there is an equivalent symbol-rate SIMO model according to Figure 7.
Finally, an algorithm for the blind *identification* of possibly mixed-phase autoregressive moving-average (ARMA) models was derived from DF-EVA and presented at the 1995 workshop on HOS [1].

4.4 Equalization of time-variant channels

So far, the transmission channel was supposed to be time-invariant. However, as EVA just requires short blocks of received data samples, it is also applicable without modification to modestly time-variant channels. Higher degrees of time-variance of the channel $h(k,\nu)$ with output sequence[14]

$$v(k) = \sum_{\nu=0}^{q} h(k,\nu)\, d(k-\nu) \tag{31}$$

do require *time-variant (TV)* equalization, however

$$x(k) = \sum_{\nu=0}^{\ell} e(k,\nu)\, v(k-\nu)\,. \tag{32}$$

In any instant of time, the overall system $h(k,\nu) *_\nu e(k,\nu)$ is linear, so that the quality criterion (8) can be applied in any instant. This leads to the generalized eigenvector problem

$$\boxed{\mathbf{C}_4^{yv}(k)\,\mathbf{e}_{\mathrm{EVA}}(k) = \lambda\,\mathbf{R}_{vv}(k)\,\mathbf{e}_{\mathrm{EVA}}(k)}\,. \qquad \textbf{“TV-EVA equation”} \tag{33}$$

The main problem with (33) is to estimate the time-variant auto-correlation and cross-cumulant matrices $\mathbf{R}_{vv}(k)$ and $\mathbf{C}_4^{yv}(k)$, respectively. This is further aggravated by the additional computational effort necessary for the solution of (33) in any time instant k. If some *a-priori* knowledge about the change of the equalizer's coefficients within a given data block is available (such as "modest" changes or cyclostationarity), the time-variant equalizer coefficients $e(k,\nu)$ can be described by a series expansion with some basis functions and few time-*in*variant coefficients.
Consider as an example the power expansion (for modest time-variance)

$$e(k,\nu) = \sum_{\mu=0}^{M-1} k^\mu e_\mu(\nu) = e_0(\nu) + k\,e_1(\nu) + k^2\,e_2(\nu) + \cdots + k^{M-1}\,e_{M-1}(\nu)\ . \tag{34}$$

[14] where k refers to the (absolute) observation time and ν denotes the time difference between the observation and excitation instants.

In this case, the overall system $s(k)$ is given by

$$s(k,\kappa) = \sum_{\nu=\min\{0,\kappa-q\}}^{\max\{\kappa,\ell\}} e(k,\nu)\cdot h(k-\nu,\kappa-\nu) = \sum_{\mu=0}^{M-1}\sum_{\nu=\min\{0,\kappa-q\}}^{\max\{\kappa,\ell\}} e_\mu(\nu)\cdot k^\mu\, h(k-\nu,\kappa-\nu) \tag{35}$$

with the equalizer output

$$x(k) = \sum_{\kappa=0}^{\ell+q} s(k,\kappa)\, d(k-\kappa)\,. \tag{36}$$

Equation (35) can be explained as follows: the output data from M different time-variant channels $h_\mu(k,\nu) = k^\mu\, h(k,\nu)$ are equalized by M time-invariant systems $e_\mu(\nu)$. To assess (instantaneous) equalization quality, we may take the cross-kurtosis quality criterion (8) in any instant of time k

$$\text{maximize} \quad |c_4^{xy}(k,0,0)| \qquad \text{subject to} \qquad r_{xx}(k,0) = \sigma_d^2\;, \tag{37}$$

where $c_4^{xy}(k,0,0)$ is defined by the right side of equation (7). As we attempt to minimize MSE (see eq. (1)) over the *entire* observation period, the quality function (37) should be considered for the *entire* range of k values. So, the *mean* cross-kurtosis may be used as a measure for equalization quality

$$\bar{c}_4^{xy}(0,0) \triangleq \frac{1}{L-\ell}\sum_{k=\ell}^{L-1} c_4^{xy}(k,0,0) \stackrel{!}{=} \max \quad \text{subject to} \quad \bar{r}_{xx}(0) \triangleq \frac{1}{L-\ell}\sum_{k=\ell}^{L-1} r_{xx}(k,0) \stackrel{!}{=} \text{const}\,. \tag{38}$$

The maximum value of (38) can be achieved, if and only if the maximum value occurs in all instants of time k, i.e. if equalization is successful.

Given the quality function (38) and the decomposition (35), the derivation of a time-variant EVA version is analogous to section 4.1. Again, we obtain a generalized eigenvector problem which determines the equalizer coefficients. The sole difference is that the elements of the matrices $\widetilde{\mathbf{C}}_4^{yv}$ and $\widetilde{\mathbf{R}}_{vv}$ are time averaged cross-cumulants $\bar{c}_4^{vy}(i_1,i_2)$ and time averaged autocorrelation coefficients $\bar{r}_{vv}(i)$. It is by far easier to estimate these mean values than the exact time-dependent values. With "TV" standing for "time-variant equalization", the resulting approach is termed TV-EVA.

5 Simulation results

In this section, we illustrate the performance of the equalization algorithms derived from GenEVA in section 4. Four simulation results based on the channel examples C3 to C6 (see Table 1) and the simulation parameters given in Table 2 are presented.

Channel example	Sampling rate	No. of coeff.	Description
C1	$1/T$	5	Synthetic channel with two maximum magnitude coefficients
C2	$1/T$	7	Synthetic channel with one maximum magnitude coefficient
C3	$2/T$	10	Critical synthetic channel (with three zeros on the unit circle)
C4	$1/T$	18	Sample multipath radio channel in a DAB *bad urban* environment
C5	$2/T$	35	Sample multipath radio channel in a DAB *bad urban* environment
C6	$1/T$	2	Synthetic time-variant channel with a zero crossing the unit circle

Table 1: Channel examples used for the simulations

Fig. no.	Modulation $d(k)$	Channel example	Number L of rec. samples	Simulation demonstrates ...
2	QPSK	C1	∞	sensitivity of EVA solution with respect to eq. (13)
3	QPSK	C2	1000, varying	quality & conv. of EVA solution for different $w(k)$
4	QPSK	C1	500	iterative adjustment of $f(k)$ and $e(k)$ by EVA
5	QPSK	C1	varying	convergence rates of EVA and RLS
6	16-QAM	C1	300, 500, 1000	EVA convergence rate
10	QPSK	C3	∞	FTS-EVA performance for $M = 2$
12	QPSK	C4	500	convergence behavior of DF-EVA and DF-MMSE
13	QPSK	C4/C5	500	SER(E_s/N_0) for different equalizer structures
14	QPSK	C6	250	tracking performance of TV-EVA

Table 2: Overview of the main simulation parameters

First, we demonstrate the asymptotic performance of FTS-EVA as described in section 4.2. Referring to Figure 8 with $M = 2$, we select the channel example C3 with an impulse response $h^{[2]}(n)$ sampled at $2/T$. Figure 10a displays the zeros of the z transform of $h^{[2]}(n)$ in the complex z-plane. As three zeros are exactly located on the unit circle, perfect equalization would *not* be possible with a symbol-rate FIR equalizer with finite order. Decomposing the noiseless received sequence $v^{[2]}(n)$ into its polyphase components $v_0(k)$ and $v_1(k)$ and using true matrices $\widetilde{\mathbf{C}}_4^{yv}$ and $\widetilde{\mathbf{R}}_{vv}$, two iterations of FTS-EVA are carried out for $\boldsymbol{\ell}_0 = \boldsymbol{\ell}_1 = [8]$ to adjust the equalizer coefficients $e^{[2]}(n)$. By the magnitude of the deconvolution result $s^{[2]}(n) = h^{[2]}(n) * e^{[2]}(n)$, Figure 10b indicates perfect equalization: with the exception of $n = 13$, all odd lag samples of $s^{[2]}(n)$ vanish so that the first Nyquist condition is met.

The following two simulation results are based on a sample multipath radio channel in a *bad urban* propagation environment defined for the European *Digital Audio Broadcasting (DAB)* project EUREKA-147 [19]. The vertical lines in Figure 11a indicate the magnitude impulse response $|h^{[2]}(n)|$ of channel example C5 sampled at $2/T$, while the dots represent an equivalent symbol-rate channel C4 with impulse response $h(k) = h^{[2]}(2k)$. Figure 11b depicts the zeros of C4 in the complex z-plane.

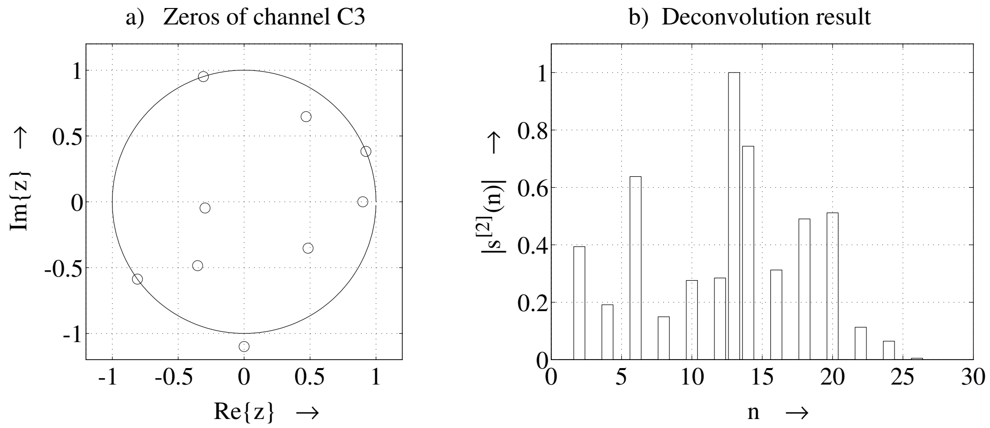

Figure 10: Asymptotic performance of FTS-EVA for double symbol-rate sampling
$d(k)$: QPSK; $h^{[2]}(n)$: C3 (three zeros on unit circle)
a) Zeros of channel C3 in the complex z-plane
b) Deconv. result $|s^{[2]}(n)|$ for $M = 2$, $L \to \infty$, $\boldsymbol{\ell}_0 = \boldsymbol{\ell}_1 = [8]$, $\boldsymbol{i} = [2]$

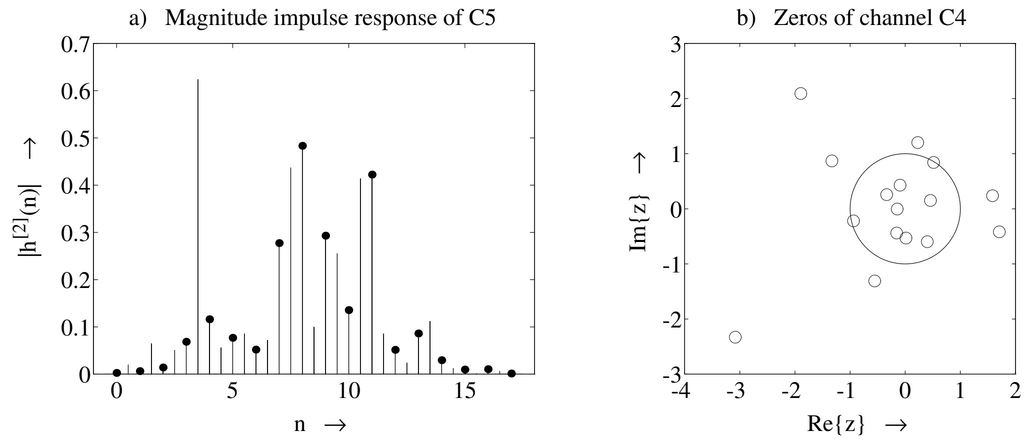

Figure 11: Sample multipath radio channel in a DAB *bad urban* propagation environment
a) Magn. impulse response $|h^{[2]}(n)|$ of channel C5 sampled at $2/T$ (lines)
Magn. impulse response $|h(k)|$ of channel C4 sampled at $1/T$ (dots)
b) Zeros of channel C4 in the complex z-plane

For the transmission of an i.i.d. QPSK sequence $d(k)$ over the channel C4, Figure 12 illustrates the performance of DF-EVA (see section 4.3) under real error conditions, where $L = 500$ samples of $v(k)$ are taken into account. In step S1 of DF-EVA, linear equalization is performed with EVA without order increase: $\boldsymbol{i} = [\mathcal{I}^{(0)}]$ iterations of EVA are executed for $\boldsymbol{\ell} = [64]$ to obtain the tentatively decided sequence $\hat{d}^{(0)}(k)$. Using $\hat{d}^{(0)}(k)$ as initial reference data, a number of $\mathcal{I} = 20$ further iterations of GENEVA with $\ell_0 = \ell_f = 16$ and $\ell_1 = \ell_b = 4$ are executed in step S2 to retrieve the final sequence $\hat{d}^{(\mathcal{I})}(k)$. From this sequence and the transmitted data $d(k)$, the *symbol error rate (SER)* is calculated. For different numbers $\mathcal{I}^{(0)}$ of iterations in step S1, SER is given in Figure 12 in terms of the iteration number. For comparison, the dotted lines are generated by replacing GENEVA in step S2 with the DF-MMSE solution (30) based on the tentatively decided sequence $\hat{d}^{(0)}(k)$.

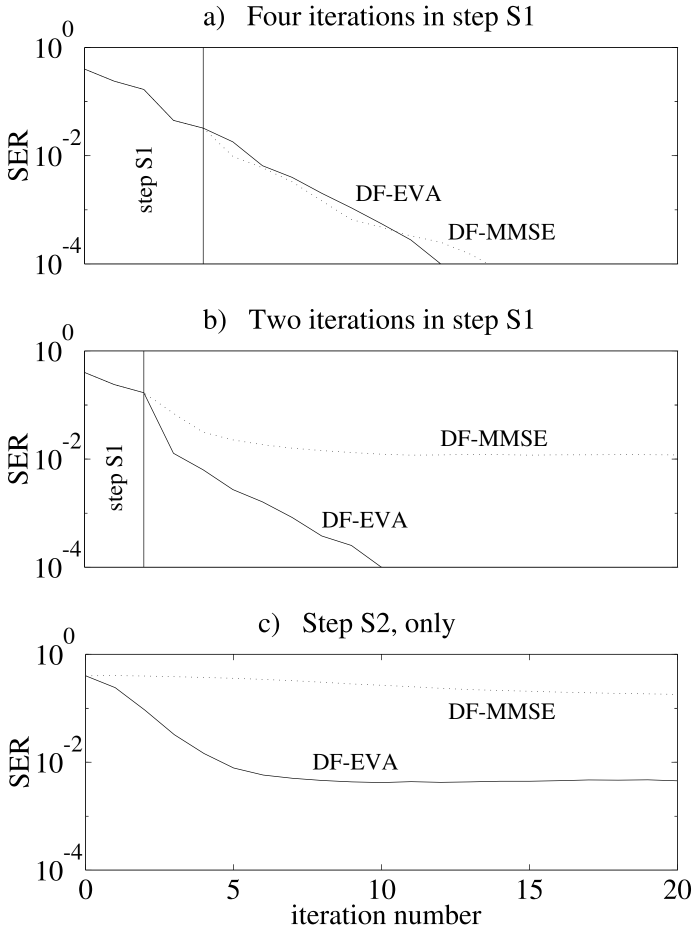

Figure 12: Convergence behavior of DF-EVA for different numbers $\mathcal{I}^{(0)}$ of iterations in step S1
$d(k)$: QPSK; $h(k)$: C4 (two zeros close to the unit circle)
DF-EVA parameters: $L = 500$, $\boldsymbol{\ell} = [64]$, $\boldsymbol{i} = [\mathcal{I}^{(0)}]$ with $\mathcal{I}^{(0)} = 4$, 2, and 0 (Fig. a,b,c),
$\ell_f = 16$, $\ell_b = 4$, $\mathcal{I} = 20$

From Figure 12a, we realize that both methods exhibit a similar convergence performance, if $\mathcal{I}^{(0)}$ is high enough ($\mathcal{I}^{(0)} = 4$ in this example) to ensure a modest initial error rate SER(4) in the order of 10^{-2} for step S2. If, however, the number of iterations is reduced to $\mathcal{I}^{(0)} = 2$ (see Fig. 12b), convergence of DF-MMSE is degraded considerably while DF-EVA still converges properly. In Fig. 12c, we consider the algorithms convergence behavior without step S1, i.e. for $\mathcal{I}^{(0)} = 0$. DF-EVA still reduces SER while DF-MMSE fails. This can be explained as follows: Without step S1, the initial error rate SER(0) is extremely high so that the decided data $\hat{d}^{(0)}(k)$ and the received sequence $v(k)$ are nearly uncorrelated. Therefore, the DF-MMSE result is completely wrong. In case of DF-EVA, however, the feedback coefficients are set to about zero because $\hat{d}^{(0)}(k)$ and the reference system output $y(k)$ are almost uncorrelated whereas the forward coefficients (the calculation of which is independent from $\hat{d}^{(0)}(k)$) are updated properly. Consequently, a proper update of the feedback coefficients begins after some iterations, when the error rate is sufficiently low. In summary, we can state that DF-EVA is robust with respect to decision errors. Further investigations reveal that a result near the optimum can be obtained even without step S1 if the data blocklength is increased (to $L = 1000$, e.g.).

For a QPSK transmission over the *bad urban* channel C4/C5, the performance levels typically achieved by the following three equalizer structures are compared in the following simulation:

- Symbol-rate FIR-(64) equalizer adjusted by EVA
- Fractional tap spacing (FTS) FIR equalizer ($M = 2$, $\boldsymbol{\ell}_0 = \boldsymbol{\ell}_1 = [8]$) adjusted by FTS-EVA
- Decision-feedback (DF) equalizer ($\ell_f = 16$, $\ell_b = 4$) adjusted by DF-EVA

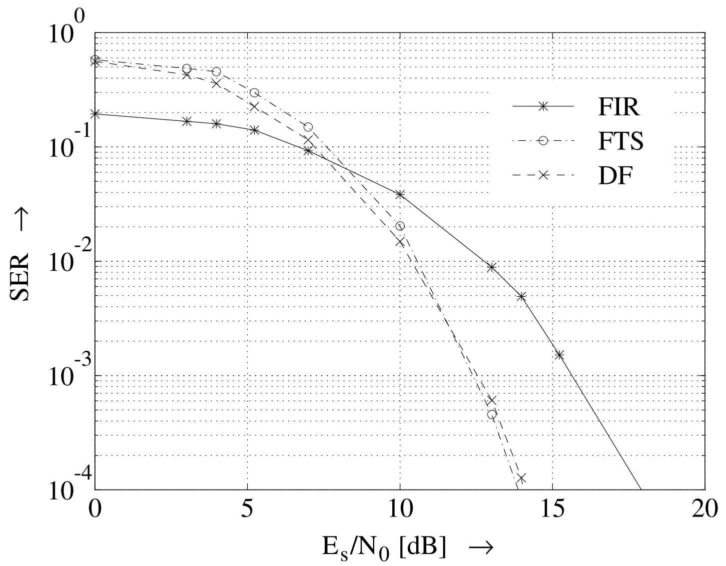

Figure 13: Symbol error rates (SER) for different equalizers adjusted by EVA or GENEVA
$d(k)$: QPSK; $h(k)/h^{[2]}(n)$: C4/C5; $n(k)$: varying E_s/N_0; $L = 500$
FIR: symbol-rate FIR equalizer adjusted by EVA: $\boldsymbol{\ell} = [4, 8, 12, \cdots, 64]$, $\boldsymbol{i} = [3, \cdots, 3]$
FTS: fractional tap spacing FIR eq. adj. by FTS-EVA: $M = 2$, $\boldsymbol{\ell}_1 = \boldsymbol{\ell}_2 = [8]$, $\boldsymbol{i} = [10]$
DF: dec.-feedb. eq. adj. by DF-EVA: $\boldsymbol{\ell} = [4, 8, 12]$, $\boldsymbol{i} = [2, 2, 2]$, $\ell_f = 16$, $\ell_b = 4$, $\mathcal{I} = 10$

$L = 500$ samples are used to estimate the required correlation and cumulant sequences. Fig. 13 shows SER in terms of the channel SNR, expressed as E_s/N_0, where E_s indicates the energy of a data symbol and N_0 denotes the power spectrum density of the additive white Gaussian noise $n(k)$. It can be seen that the DF and FTS equalizers outperform the symbol-rate FIR equalizer for $E_s/N_0 > 7.5$ dB, while the latter is superior in SER in low SNR environments.

We conclude this section with the equalization of a time-variant channel, where TV-EVA introduced in section 4.4 is applied. As a channel model, we apply the first order system C6

$$h(k,t) = \delta(k) - z_0(t)\,\delta(k-1)\,, \qquad \text{where} \qquad z_0(t) = 0.001 e^{j} \cdot t/T \quad \text{for} \quad t = 0, \cdots, 2000\,T$$

with a zero $z_0(t)$ moving uniformly from $z_0 = 0$ to $z_0 = 2e^{j}$. Aligned with the time axis of Figure 14, some instantaneous zero locations are given in small complex planes on top of this Figure. Using blocks of $L = 250$ samples to adjust the $\ell + 1 = 17$ equalizer coefficients, Figure 14 shows the gliding mean square error $\text{MSE} = \sum |x(k) - d(k - k_0)|^2 / L$ for three algorithms used to update the coefficients: *(i)* time-invariant MMSE-(ℓ) solution (2) (dotted), *(ii)* TV-EVA-(ℓ) solution (solid, $M = 1$), and *(iii)* time-variant MMSE-(ℓ) solution (dashed, $M = 1$). The latter can be obtained if $x(k)$ according

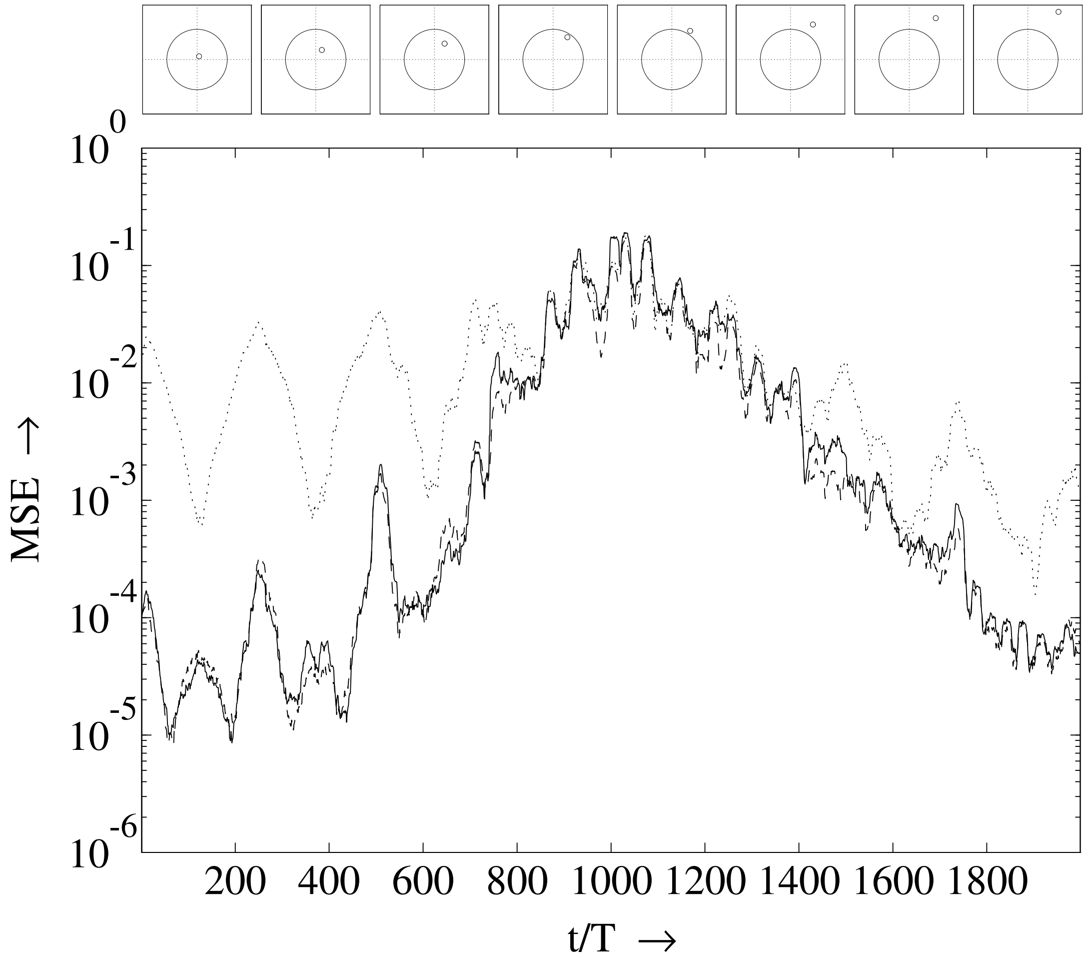

Figure 14: TV-EVA equalization of a time-variant channel
$d(k)$: QPSK; $h(k,t)$: C6 (one zero crossing the unit circle); $L = 250$, $\ell = 16$
TV-EVA (solid) par.: $\boldsymbol{\ell} = [4, 8, 12, 16]$, $\boldsymbol{i} = [2, 2, 2, 2]$; $M = 1$, $\mathcal{I} = 20$
TV-MMSE (dashed) parameters: $M = 1$
Time-invariant MMSE (dotted)

to (36) and (35) is inserted into the above "block" MSE quality function. Its optimization yields

$$\tilde{\mathbf{e}}_{\mathrm{MMSE}}(k) = \left(\widetilde{\mathbf{R}}_{vv}(k)\right)^{-1} \tilde{\mathbf{r}}_{vd}(k) \qquad \text{with} \qquad \begin{cases} \tilde{\mathbf{r}}_{vd}(k) & \stackrel{\Delta}{=} \tilde{\mathbf{V}}_k^* \cdot \mathbf{d}_k \\ \widetilde{\mathbf{R}}_{vv}(k) & \stackrel{\Delta}{=} \tilde{\mathbf{V}}_k^* \tilde{\mathbf{V}}_k \end{cases} \tag{39}$$

where $\tilde{\mathbf{e}}_{\mathrm{MMSE}}(k)$ is defined analogously to $\mathbf{e}_{\mathrm{EVA}}(k)$ in (33) and the matrix $\tilde{\mathbf{V}}_k = [\mathbf{V}, \mathbf{V}_1]$ contains the received sequence $v(k)$ where in $\mathbf{V}_1$, each row is multiplied by its row index.

We realize that the time-variant solutions deliver smaller values of MSE than the time-invariant approaches. Moreover, TV-EVA approximates the time-variant MMSE solution, which is the optimum linear solution for $M = 1$. In the range of $800 \leq t/T \leq 1300$, all equalizers exhibit a rather poor performance due to the fact that the channel zero is close to the unit circle and the order of the equalizers is limited to $\ell = 16$.

6 Conclusions

We have introduced two fast algorithms for the blind equalization of frequency selective possibly mixed-phase linear transmission channels. The first approach, termed EVA, adjusts a symbol-rate FIR equalizer and achieves optimum linear equalization from few samples of the received signal so that it can be applied to slowly time-varying channels, too. For constant modulus signals, the *blind* EVA approach was shown to converge as fast as the *non-blind* RLS algorithm.
The generalized algorithm GENEVA is capable of adjusting the coefficients of *(i)* multiple parallel symbol-rate FIR equalizers, *(ii)* fractional tap spacing FIR equalizers, *(iii)* non-linear decision-feedback equalizers and *(iv)* combinations thereof. Based on a model to describe the time-variant behavior of the equalizer coefficients, it can even be applied to *(v)* fast time-varying channels.

Remark: MATLAB programs implementing EVA and GENEVA as well as postscript files of preprints of related publications are readily available from our WWW server (`http://www.comm.uni-bremen.de`).

Acknowledgements

We would like to express our gratitude to the anonymous reviewers for having compiled comprehensive and thorough reviews leading to numerous modifications throughout the paper. We also thank the reviewers for their patience with respect to a considerable delay in the revision process due to changes of affiliation of all authors.

Appendices

A Estimation of the matrices $\mathbf{R}_{vv}$ and $\mathbf{C}_4^{yv}$

From a block of L received data samples $v(0), \cdots, v(L-1)$, consistent estimates $\widehat{\mathbf{R}}_{vv}$ and $\widehat{\mathbf{C}}_4^{yv}$ used in the EVA equation (12) in place of $\mathbf{R}_{vv}$ and $\mathbf{C}_4^{yv}$, respectively, can be calculated according to[15]

$$\widehat{\mathbf{R}}_{vv} \triangleq \frac{1}{L-\ell} \sum_{k=\ell}^{L-1} \mathbf{v}_k \mathbf{v}_k^* \qquad \text{with} \qquad \mathbf{v}_k^* \triangleq [v(k), v(k-1), \cdots, v(k-\ell)] \tag{A.1}$$

and

$$\begin{aligned}\widehat{\mathbf{C}}_4^{yv} \triangleq\ & \frac{1}{L-\ell}\left(\sum_{k=\ell}^{L-1} |y(k)|^2\, \mathbf{v}_k\, \mathbf{v}_k^*\right) - \frac{1}{(L-\ell)^2}\left[\left(\sum_{k=\ell}^{L-1} |y(k)|^2\right)\cdot\left(\sum_{k=\ell}^{L-1} \mathbf{v}_k\, \mathbf{v}_k^*\right)\right. \\ & \left. + \left(\sum_{k=\ell}^{L-1} \mathbf{v}_k\, y^*(k)\right)\cdot\left(\sum_{k=\ell}^{L-1} \mathbf{v}_k^*\, y(k)\right) + \left(\sum_{k=\ell}^{L-1} \mathbf{v}_k\, y(k)\right)\cdot\left(\sum_{k=\ell}^{L-1} \mathbf{v}_k^*\, y^*(k)\right)\right] .\end{aligned} \tag{A.2}$$

Note that these are "RLS-type" unbiased sample averages. For example, the values on any given diagonal of $\widehat{\mathbf{R}}_{vv}$ are *not* identical, so that $\widehat{\mathbf{R}}_{vv}$ is non-Toeplitz – as opposed to the true matrix $\mathbf{R}_{vv}$.

B Robustness of RLS with respect to correlation estimation errors

From Figure 5, we realize that both RLS and EVA achieve excellent equalization qualities from as few as $L = 150$ samples, although neither the cumulants nor the correlation coefficients can be estimated with sufficient accuracy. In the noiseless case, this robustness with respect to correlation and cumulant estimation errors can be explained by the following effect [13].

RLS solves the normal equation $\widehat{\mathbf{R}}_{vv}\mathbf{e} = \widehat{\mathbf{r}}_{vd}$ (cf. eq. (2)). On the left side of this system of equations, the estimate $\widehat{\mathbf{R}}_{vv}$ according to (A.1) is applied

$$\widehat{\mathbf{R}}_{vv}\, \mathbf{e} = \frac{1}{L-\ell} \sum_{k=\ell}^{L-1} \mathbf{v}_k\, \mathbf{v}_k^*\, \mathbf{e} = \frac{1}{L-\ell} \sum_{k=\ell}^{L-1} \mathbf{v}_k\, x(k) \qquad \text{with} \qquad x(k) = \mathbf{v}_k^*\, \mathbf{e}\ , \tag{B.1}$$

while on the right side, the cross-correlation vector $\widehat{\mathbf{r}}_{vd}$ is calculated by

$$\widehat{\mathbf{r}}_{vd} = \frac{1}{L-\ell} \sum_{k=\ell}^{L-1} \mathbf{v}_k\, d(k-k_0)\ . \tag{B.2}$$

On the assumption of perfect equalization (i.e. $x(k) \equiv d(k-k_0)$), we realize that equations (B.1) and (B.2) are identical. Thus, the solution of the system of equations is *independent from the quality of the correlation estimates*. This gives an insight into the robustness of RLS with respect to estimation errors in the correlation coefficients. EVA's robustness will be clarified in Appendices C and D.

[15] these equations are obtained if $c_4^{xy}(0,0)$ and $r_{xx}(0)$ in (8) are estimated by unbiased sample averaging.

C Robustness of EVA to correlation and cumulant estimation errors

In Appendix B, justification was given for the robustness of RLS with respect to correlation estimation errors. For *constant modulus* modulation schemes such as *Phase Shift Keying (PSK)*, a similar effect causes EVA to be robust to estimation errors in the correlation and cumulant estimates [13].

Regarding the EVA equation $\lambda\widehat{\mathbf{R}}_{vv}\mathbf{e} = \widehat{\mathbf{C}}_4^{yv}\mathbf{e}$, the left side is proportional to (B.1). As for the right side, the estimate $\widehat{\mathbf{C}}_4^{yv}$ according to (A.2) can be simplified for modulation schemes with a probability density function $p_d(\theta)$ satisfying the symmetry condition $p_d(\theta) = p_d(j\theta)$. For example, this is true for all kinds of PSK and *QAM (Quadrature Amplitude Modulation)* signals. It leads to $\bar{r}_{dd}(i) = E\{d(k)d(k+i)\} = 0$, so that the third expression in (A.2) vanishes. The right side of the EVA equation can be rewritten as

$$\begin{aligned}\widehat{\mathbf{C}}_4^{yv}\mathbf{e} &= \frac{1}{L-\ell}\left(\sum_{k=\ell}^{L-1}|y(k)|^2\,\mathbf{v}_k\,x(k)\right)\\ &\quad -\frac{1}{(L-\ell)^2}\left[\left(\sum_{k=\ell}^{L-1}|y(k)|^2\right)\left(\sum_{k=\ell}^{L-1}\mathbf{v}_k\,x(k)\right)+\left(\sum_{k=\ell}^{L-1}\mathbf{v}_k\,y(k)\right)\left(\sum_{k=\ell}^{L-1}x(k)\,y^*(k)\right)\right], \qquad \text{(C.1)}\end{aligned}$$

where $x(k)$ was substituted for $\mathbf{v}_k^*\,\mathbf{e}$. Assuming that perfect equalization is possible (noiseless case), both $x(k)$ and $y(k)$ will approach $d(k-k_m)$ after some EVA iterations: Thus, if we replace $x(k)$ and $y(k)$ in (C.1) with $d(k-k_m)$ while recalling that for constant modulus signals we have $|d(k-k_m)|^2 = \sigma_d^2$, we obtain

$$\begin{aligned}\widehat{\mathbf{C}}_4^{yv}\mathbf{e} &= \frac{1}{L-\ell}\left(\sum_{k=\ell}^{L-1}\sigma_d^2\,\mathbf{v}_k\,d(k-k_m)\right)-\frac{2}{(L-\ell)^2}\underbrace{\left(\sum_{k=\ell}^{L-1}\sigma_d^2\right)}_{=(L-\ell)\cdot\sigma_d^2}\left(\sum_{k=\ell}^{L-1}\mathbf{v}_k\,d(k-k_m)\right)\\ &= -\frac{\sigma_d^2}{L-\ell}\left(\sum_{k=\ell}^{L-1}\mathbf{v}_k\,d(k-k_m)\right) = -\sigma_d^2\,\frac{1}{L-\ell}\left(\sum_{k=\ell}^{L-1}\mathbf{v}_k\,x(k)\right). \qquad \text{(C.2)}\end{aligned}$$

Up to a factor, this is identical with the left side of the EVA equation (cf. eq. (B.1)). Therefore, the solution of the EVA equation is *independent from the quality of the estimates* $\widehat{\mathbf{R}}_{vv}$ and $\widehat{\mathbf{C}}_4^{yv}$ according to (A.1) and (A.2). This explains the robustness of EVA to correlation and cumulant estimation errors.

This consideration does not apply to amplitude modulation schemes, because $|d(k-k_m)|^2 = \sigma_d^2$ is not satisfied with such signals.

D Influence of the kurtosis quality function on QAM signals

According to Appendix C, EVA's robustness to correlation and cumulant estimation errors does not apply to amplitude modulation schemes such as 16-QAM used for Figure 6. In the left subplot of Fig. 6 ($L = 300$), the equalizer output signal $x(k)$ seems to thin out for small and large magnitudes. We will explain in this appendix that this is caused by EVA's quality function.

After some EVA iterations, $x(k)$ and $y(k)$ are virtually identical, so that the cross-kurtosis quality function (8) can be rewritten in terms of the normalized kurtosis K of the equalizer output $x(k)$

$$K \triangleq \frac{|c_4^{xx}(0,0)|}{(r_{xx}(0))^2} = \operatorname{sgn}\{\gamma_4^d\}\cdot\left(\frac{E\{|x(k)|^4\}-2(E\{|x(k)|^2\})^2-|E\{x^2(k)\}|^2}{(E\{|x(k)|^2\})^2}\right)$$

$$= \quad \operatorname{sgn}\{\gamma_4^d\} \cdot \left(\frac{E\{|x(k)|^4\}}{(E\{|x(k)|^2\})^2} - 2 \right) \stackrel{!}{=} \max\,, \tag{D.1}$$

where "sgn" represents the sign operator and $E\{x^2(k)\}$ vanishes for QAM signals. Replacing statistical expectation with unbiased sample averages, we obtain the estimated normalized kurtosis

$$\hat{K} = \operatorname{sgn}\{\gamma_4^d\} \cdot \left(\frac{(L-\ell)\sum_{k=\ell}^{L-1} |x(k)|^4}{(\sum_{k=\ell}^{L-1} |x(k)|^2)^2} - 2 \right), \tag{D.2}$$

which is maximized by EVA. Note that $\hat{K}$ is rotationally invariant, i.e. all samples $x(k)$ with equal magnitudes are assigned equal weights. The individual weight, which is assigned to each sample $x(\mu)$ can be derived from the difference between $\hat{K}$, which is based on $L-\ell$ samples, and $\hat{K}_\mu$ where the sample $x(\mu)$ is omitted

$$\Delta\hat{K}(x(\mu)) = \hat{K} - \hat{K}_\mu = \operatorname{sgn}\{\gamma_4^d\} \left(\frac{(L-\ell)\sum_{k=\ell}^{L-1} |x(k)|^4}{(\sum_{k=\ell}^{L-1} |x(k)|^2)^2} - \frac{(L-\ell)\sum_{k=\ell,k\neq\mu}^{L-1} |x(k)|^4}{(\sum_{k=\ell,k\neq\mu}^{L-1} |x(k)|^2)^2} \right). \tag{D.3}$$

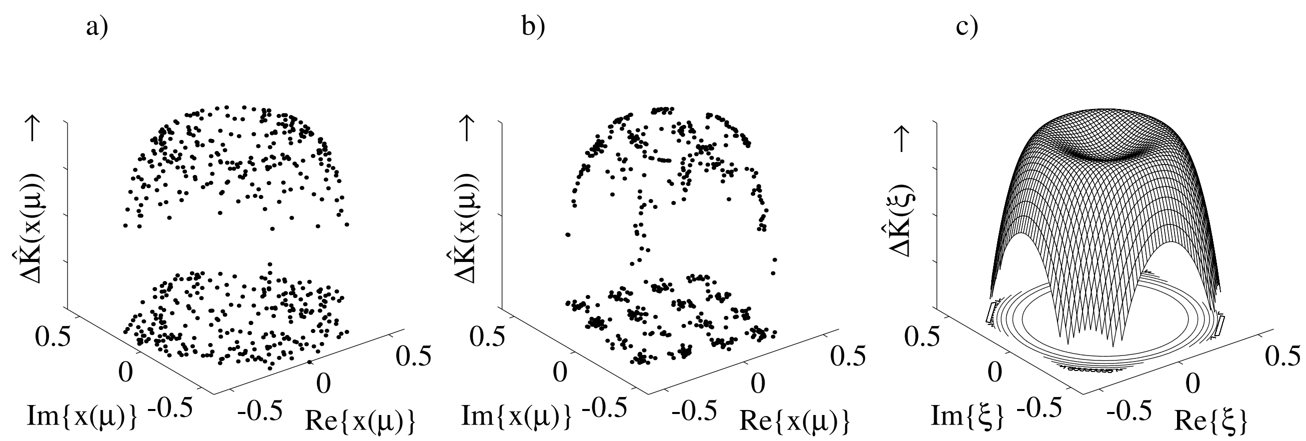

Figure 15: Individual weights attributed to the equalized data by the quality function
a) Individual weights $\Delta\hat{K}$ for the equalized data $x(\mu)$ from Figure 6 ($L = 300$)
b) Individual weights $\Delta\hat{K}$ for the equalized data $x(\mu)$ from Figure 6 ($L = 1000$)
c) Individual weights $\Delta\hat{K}$ for a varying value ξ of $x(\mu)$

In Figure 15a,b, the equalized sequences $x(\mu)$ shown in the complex plane in the left and right subplots of Fig. 6 are drawn in the floor planes of the 3D plots. The individual weights attributed by $\Delta\hat{K}(x(\mu))$ to each sample $x(\mu)$ are displayed on the z axis. For a short blocklength ($L = 300$, see Fig. 15a) and a relatively high equalizer order ($\ell = 32$), obviously, it is advantageous for a high total value of $\hat{K}$ to generate a distorted sequence with almost constant magnitude rather than a well equalized sequence with non-constant amplitude (such as that displayed in the floor plane of Fig. 15b).

To obtain the smooth surface in Figure 15c, the second fraction in (D.3) is kept constant by suppressing the same sample $x(\mu)$ for all values shown on the z axis. If we overwrite this sample $x(\mu)$, in the first fraction of (D.3), by a complex value ξ, and calculate $\Delta\hat{K}$ for each value ξ in the complex plane, we gain the function $\Delta\hat{K}(\xi)$ displayed in Fig. 15c. Clearly, the max. value of the kurtosis quality function would be achieved if $x(\mu)$ was located on a circle, i.e. if the equalizer output had a constant envelope. This explains the optimum adjustment of the equalizer for constant modulus signals (cf. Appendix C).

References

[1] D. Boss, B. Jelonnek, and K.D. Kammeyer. Decision-Feedback Eigenvector Approach to Blind ARMA Equalization and Identification. In *Proc. IEEE-SP/ATHOS Workshop on Higher-Order Statistics*, pages 320–324, Begur, Spain, June 1995.

[2] D. Boss, B. Jelonnek, and K.D. Kammeyer. Eigenvector Algorithm for Blind MA System Identification. *Elsevier Signal Processing*, 66(1), April 1998.

[3] D. Boss and K.D. Kammeyer. Blind Identification of Mixed-Phase FIR Systems with Application to Mobile Communication Channels. In *Proc. ICASSP-97*, volume 5, pages 3589–3592, Munich, Germany, April 1997.

[4] J.-F. Cardoso and B. H. Laheld. Equivariant Adaptive Source Separation. *IEEE Trans. on Signal Processing*, SP-44(12):3017–3030, December 1996.

[5] J.-F. Cardoso and A. Souloumiac. An Efficient Technique for Blind Separation of Complex Sources. In *Proc. IEEE Signal Proc. Workshop on Higher-Order Statistics*, pages 275–279, South Lake Tahoe, California, June 1993.

[6] J.-F. Cardoso and A. Souloumiac. Blind Beamforming for non-Gaussian Signals. *Proceedings of the IEE-F*, 140(6):362–370, December 1993.

[7] Z. Ding. Characteristics of Band-Limited Channels Unidentifiable from Second-Order Cyclostationary Statistics. *IEEE Signal Processing Letters*, SPL-3(5):150–152, May 1996.

[8] D. Donoho. On minimum entropy deconvolution. *Proc. 2nd Appl. Time Series Symposium*, pages 565–608, 1980.

[9] W. A. Gardner. *Introduction to Random Processes: with Applications to Signals and Systems.* McGraw-Hill, New York, second edition, 1989.

[10] D. N. Godard. Self-Recovering Equalization and Carrier Tracking in Two-Dimensional Data Communication Systems. *IEEE Trans. on Communications*, Com-28(11):1867–1875, November 1980.

[11] G. H. Golub and C. F. Van Loan. *Matrix Computations.* The John Hopkins University Press, London and Baltimore, MD, second edition, 1989.

[12] S. Haykin. *Adaptive Filter Theory.* Prentice-Hall, Upper Saddle River, New Jersey 07458, third edition, 1996.

[13] B. Jelonnek. *Referenzdatenfreie Entzerrung und Kanalschätzung auf der Basis von Statistik höherer Ordnung.* PhD thesis, Dept. of Telecommunications, Hamburg University of Technology, Hamburg, Germany, March 1995.

[14] B. Jelonnek and K.D. Kammeyer. A Blind Adaptive Equalizer based on a Lattice/All-pass Configuration. In *Proc. EUSIPCO-92*, volume II, pages 1109–1112, Brussels, Belgium, August 1992.

[15] B. Jelonnek and K.D. Kammeyer. Eigenvector Algorithm for Blind Equalization. In *Proc. IEEE Signal Proc. Workshop on Higher-Order Statistics*, pages 19–23, South Lake Tahoe, California, June 1993.

[16] B. Jelonnek and K.D. Kammeyer. A Closed-Form Solution to Blind Equalization. *Elsevier Signal Processing*, 36(3):251–259, April 1994. Special Issue on Higher Order Statistics.

[17] K.D. Kammeyer and B. Jelonnek. A New Fast Algorithm for Blind MA-System Identification based on Higher Order Cumulants. In *Proc. SPIE Advanced Signal Proc.: Algorithms, Architectures and Implementations V*, volume 2296, pages 162–173, San Diego, California, July 1994.

[18] K.D. Kammeyer, R. Mann, and W. Tobergte. A Modified Adaptive FIR Equalizer for Multipath Echo Cancellation in FM Transmission. *IEEE Journal on Selected Areas in Communications*, 5:226–237, 1987.

[19] K.D. Kammeyer, U. Tuisel, H. Schulze, and H. Bochmann. Digital Multicarrier-Transmission of Audio Signals over Mobile Radio Channels. *European Trans. on Telecommunication*, 3(3):243–254, 1992.

[20] J. M. Mendel. Use of Higher-Order Statistics in Signal Processing and System Theory: An Update. *Advanced Algorithms and Architectures for Signal Processing III*, 975:126–144, 1988.

[21] J. M. Mendel. Tutorial on Higher-Order Statistics (Spectra) in Signal Processing and System Theory: Theoretical Results and Some Applications. *Proceedings of the IEEE*, 79(3):278–305, March 1991.

[22] P. Monsen. Feedback Equalization for Fading Dispersive Channels. *IEEE Trans. on Information Theory*, IT-17:56–64, 1971.

[23] M. Mouly and M.-B. Pautet. *The GSM System for Mobile Communications.* Published by the authors, Palaiseau, France, 1992.

[24] C. L. Nikias and J. M. Mendel. Signal Processing with Higher-Order Spectra. *IEEE Signal Processing Magazine*, 10:10–37, July 1993.

[25] C. L. Nikias and M. R. Raghuveer. Bispectrum Estimation: A Digital Signal Processing Framework. *Proceedings of the IEEE*, 75(7):869–891, July 1987.

[26] J. G. Proakis. *Digital Communications.* McGraw-Hill, New York, third edition, 1995.

[27] S. U. H. Qureshi. Adaptive Equalization. *Proceedings of the IEEE*, 73(9):1349–1387, September 1985.

[28] Robinson and Enders. *Multichannel Time Series Analysis with Digital Computer Programs.* Prentice-Hall, Englewood Cliffs, New Jersey 07632, 1988.

[29] Y. Sato. A Method of Self-Recovering Equalization for Multilevel Amplitude-Modulation Systems. *IEEE Trans. on Communications*, COM-23:679–682, June 1975.

[30] O. Shalvi and E. Weinstein. New Criteria for Blind Deconvolution of Nonminimum Phase Systems (Channels). *IEEE Trans. on Information Theory*, IT-36(2):312–321, March 1990.

[31] O. Shalvi and E. Weinstein. Super-Exponential Methods for Blind Deconvolution. *IEEE Trans. on Information Theory*, 39(2):504–519, March 1993.

[32] L. Tong, G. Xu, and T. Kailath. Necessary and Sufficient Conditions of Channel Identifiability Based on Second-Order Cyclostationary Statistics. In *Proc. IEEE Int. Symp. on Info. Theory*, page 188, San Antonio, Texas, January 1993.

[33] J. R. Treichler and B. G. Agee. A new approach to multipath correction of constant modulus signals. *IEEE Trans. on Acoustics, Speech and Signal Processing*, ASSP-31:459–471, 1983.

[34] J. K. Tugnait. On Blind Identifiability of Multipath Channels Using Fractional Sampling and Second-Order Cyclostationary Statistics. *IEEE Trans. on Information Theory*, IT-41(1):308–311, January 1995.

[35] G. Ungerboeck. Fractional Tap Spacing Equaliser and Consequences for Clock Recovery in Data Modems. *IEEE Trans. on Communications*, COM-24(8):856–867, 1976.

[36] A. T. Walden. Non-Gaussian Reflectivity, Entropy, and Deconvolution. *Geophysics*, 50(12):2852–2887, 1985.

[37] K. Wesołowski. On Acceleration of Adaptive Blind Equalization Algorithms. *Archiv für Elektronik und Übertragungstechnik (AEÜ) – Int. Journal of Electronics and Communications*, 46(6):392–399, 1992.

[38] B. Widrow and S. D. Stearns. *Adaptive Signal Processing.* Prentice-Hall, Englewood Cliffs, New Jersey 07632, 1985.